Chaos

Estimate of the average timing for strong El Niño events using the recharge oscillator model with a multiplicative perturbation

Cite as: Chaos **28**, 103118 (2018); https://doi.org/10.1063/1.5030413
Submitted: 21 March 2018 . Accepted: 27 September 2018 . Published Online: 24 October 2018

Marco Bianucci, Antonietta Capotondi, Silvia Merlino, and Riccardo Mannella

openaccess

View Online Export Citation CrossMark

ARTICLES YOU MAY BE INTERESTED IN

Analysis of Shannon-Fisher information plane in time series based on information entropy
Chaos: An Interdisciplinary Journal of Nonlinear Science **28**, 103107 (2018); https://doi.org/10.1063/1.5023031

Existence and stability of chimera states in a minimal system of phase oscillators
Chaos: An Interdisciplinary Journal of Nonlinear Science **28**, 103121 (2018); https://doi.org/10.1063/1.5044750

The Jacobi diffusion process as a neuronal model
Chaos: An Interdisciplinary Journal of Nonlinear Science **28**, 103119 (2018); https://doi.org/10.1063/1.5051494

AIP Publishing

© 2018 Author(s).

Estimate of the average timing for strong El Niño events using the recharge oscillator model with a multiplicative perturbation

Marco Bianucci,[1,a)] Antonietta Capotondi,[2,3] Silvia Merlino,[1] and Riccardo Mannella[4]
[1]*Istituto di Scienze Marine, Consiglio Nazionale delle Ricerche (ISMAR - CNR), Lerici, La Spezia 19032, Italy*
[2]*CIRES, University of Colorado, Boulder, Colorado 80309, USA*
[3]*Physical Sciences Division, Earth System Research Laboratory, NOAA, Boulder, Colorado 80305, USA*
[4]*Physics Department, Pisa University, Pisa, Pisa 56126, Italy*

(Received 21 March 2018; accepted 27 September 2018; published online 24 October 2018)

El Niño Southern Oscillation (ENSO) is the leading mode of tropical Pacific variability at interannual timescales. Through atmospheric teleconnections, ENSO exerts large influences worldwide, so that improved understanding of this phenomenon can be of critical societal relevance. Extreme ENSO events, in particular, have been associated with devastating weather events in many parts of the world, so that the ability to assess their frequency and probability of occurrence is extremely important. In this study, we describe the ENSO phenomenon in terms of the Recharge Oscillator Model perturbed by multiplicative deterministic chaotic forcing, and use methodologies from the field of Statistical Mechanics to determine the average time between El Niño events of given strengths. This is achieved by describing the system in terms of its probability density function, which is governed by a Fokker Planck equation, and then using the Mean First Passage Time technique for the determination of the mean time between extreme events. The ability to obtain analytical solutions to the problem allows a clear identification of the most relevant model parameters for controlling the frequency of extreme events. The key parameter is the strength of the multiplicative component of the stochastic perturbation, but the decorrelation timescale of the stochastic forcing is also very influential. Results obtained with this approach suggest an average waiting time between extreme events of only some tens of years. © *2018 Author(s). All article content, except where otherwise noted, is licensed under a Creative Commons Attribution (CC BY) license (http://creativecommons.org/licenses/by/4.0/).* https://doi.org/10.1063/1.5030413

Improving the knowledge of the key factors that determine the features of the dynamics and of the statistics of the ENSO has very broad implications for people involved in Climate Changes study, and predictability of the large scale Ocean dynamics. Here, using standard methods of Statistical Mechanics, adapted to the case of the Recharge Oscillator Model perturbed by a multiplicative fast chaotic forcing, we characterize the timing of El Niño events and we get an analytical expression in good agreement with observations. In particular, we exploit recent results on the perturbation projection approach to dynamical systems to obtain a Fokker Planck Equation for the Probability Density Function of the ENSO events, from which, standard First Passage Time techniques lead us to the timing between ENSO events. Noticeable is the fact that for very strong ENSO events this timing is just some tens of years (about the human average lifetime), with important implications for society. This fact is a direct consequence of the non-Gaussian features of the ENSO statistics that, in turn, is strongly related to the multiplicative nature of the fast forcing of the Recharge Oscillator Model.

I. INTRODUCTION

Due to its large global impacts,[1] understanding and predicting ENSO is of critical importance in the climate community. The onset and evolution of ENSO events rely on complex ocean-atmosphere interactions in the equatorial Pacific, as well as extra-equatorial influences, leading to a large diversity in amplitude, spatial pattern, and temporal evolution of ENSO events.[2]

In spite of this complexity, simple dynamical paradigms (or Low Order Models—LOM) have been able to describe the basic features of ENSO by capturing essential aspects of the system (see Ref. 3).

In particular, the "recharge oscillator" model (ROM)[4,5] focuses on the recharge/discharge of the equatorial Pacific upper-ocean warm water volume. This process appears to be a robust feature of ENSO in both observations[6] and climate models,[7] as well as across the diversity of ENSO events, albeit with different intensities.[8,9] The recharge/discharge processes involve the interactions between sea surface temperature (SST), equatorial wind stress, and thermocline depth anomalies: a positive SST anomaly in the eastern Pacific induces westerly wind anomalies in the central Pacific, resulting in a reduced zonal gradient of thermocline depth. The changes in the zonal slope of the thermocline are associated, in turn, with anomalous meridional flow which discharges warm water from the equatorial thermocline during El Niño events, and recharges the equatorial thermocline during La Niña events.

Apart from the deterministic component of the wind stress anomalies, which is associated with the large-scale SST anomalies, stochastic wind variations in the form of

a)marco.bianucci@cnr.it

 © Author(s) 2018.

Westerly Wind Events (WWEs) provide an important triggering influence on ENSO events.[10,11] Several recent studies have shown that WWEs are often associated with the Madden Julian Oscillation (MJO):[12] WWEs are more likely to occur in the presence of warm SST conditions (see for example, among others, Refs. 13–15). This suggests that the WWEs should be seen as a state-dependent "atmospheric noise," namely, a *multiplicative*, rather than additive, forcing. It is worth stressing that, in general, multiplicative (instead of additive) fast forcings typically emerge from perturbation approaches to large-scale ocean dynamics.[16,17]

A representation of this state-dependent noise has been included in the recharge oscillator model by Jin *et al.*[18] and Levine and Jin.[19] These studies have adopted a second-order closure for the state-dependent term. An alternative approach for the inclusion of fast state-dependent perturbations to the recharge oscillator model is the projective method of Bianucci,[20–23] adapted to the ROM case[24] (B_16 hereafter), where the system is described in terms of its Probability Density Function (PDF) governed by a Fokker-Planck Equation (FPE), for which analytical solutions can be obtained. B_16 has derived some key aspects of the system statistics using this approach, including an analytical expression for the stationary PDF and a closed set of equations of motion for the first and the second moments of the ROM.

In this study, we extend the results of B_16 to examine the average time between events of a given amplitude, by using the mean First Passage Time (FPT) technique, a method stemming from the field of statistical mechanics. This quantity, for which an analytical expression can be determined, is of particular interest in the case of extreme events. Given the devastating impacts of such events, information of their expected frequency would be extremely valuable to society.

The FPT approach is applied to the one-dimensional FPE of the variable SST. This one-dimensional FPE has been obtained in B_16 from the two dimensional FPE describing the ROM, under the reasonable ansatz of a factorization of the equilibrium distribution, with the aim of obtaining an approximate analytical expression for the stationary reduced PDF of the anomalous SST. We will discuss whether the same ansatz is appropriate for evaluating the FPT of rare events, which strongly depends on the dynamical features of the process (and not only on the stationary PDF) and on the details of the PDF tails. Numerical solutions are also obtained to validate the analytical ones.

It is worth mentioning that the "non-normal" growth of fluctuations, which characterizes strong El Niño events,[25] can be explained also in terms of *multivariate* linear models with *multivariate additive* stochastic perturbations.[26,27] However, here, we focus on a *simple* ROM with a *state-dependent* perturbation, a model that, as we have already stressed, has a clearer physical motivation. Probably, a more realistic modeling of ENSO should merge this two pictures (multidimensionality and nonlinearities). However, a deeper discussion about the affective and respective roles of the dimension and of the nonlinearities of a LOM to model the complexity of ENSO goes beyond the task of the present work.

II. THE DYNAMICAL MODEL AND THE FPE

According to what we stated in the Introduction, like in B_16 we are interested to the ROM weakly forced by a very general fast deterministic system, the latter being described by some variables ξ and $\boldsymbol{\pi}$, variables which in turn obey some generic differential equations

$$\begin{aligned} \dot{h} &= -\omega T, \\ \dot{T} &= \omega h - \lambda T + \epsilon\, \xi(1+\beta T), \end{aligned} \tag{1}$$

$$\begin{aligned} \dot{\xi} &= F(\xi, \boldsymbol{\pi}), \\ \dot{\boldsymbol{\pi}} &= \boldsymbol{Q}(\xi, \boldsymbol{\pi}), \end{aligned} \tag{2}$$

where the dot denotes a time derivative (d/dt) and bold case is used for vectors. As in Ref. 18, 19, and 28, the ROM variables T and h are the equatorial east Pacific Ocean anomalous SST and the zonally averaged anomalous thermocline depth, respectively, normalized by their respective average amplitudes; the only remaining physical dimension will be time, measured in months. The parameter ω is the "free" oscillation frequency of the unperturbed system, while $1/\lambda$ is the relaxation time of the variables of the "slow manifold" as discussed in Refs. 4, 5, and 28.

Using the terminology of the projection approach of Grigolini and Bianucci[21,29,30] the ROM is viewed as the "system of interest" (or system a); $(\xi, \boldsymbol{\pi})$ represent the *booster* system (or "rest of the system" or system b), a set of general chaotic and fast variables (e.g., the MJO and WWB[31–35]) which perturb the ROM and trigger the El Niño/La Niña phenomena: these variables obey some *unspecified* equations of motion expressed by the generic functions $F(\xi, \boldsymbol{\pi})$ and $\boldsymbol{Q}(\xi, \boldsymbol{\pi})$. The value of the parameter ϵ determines the intensity of the ROM perturbation. For $\epsilon = 0$, Eq. (1) defines the unperturbed system of interest, that can also be defined "the unperturbed ROM."

In general, the interaction between the ROM and the booster should be bi-directional, implying that the booster equation of motion should be affected by the dynamics of the ROM: $F = F(\xi, \boldsymbol{\pi}, \epsilon R[h,T])$ and $\boldsymbol{Q} = \boldsymbol{Q}(\xi, \boldsymbol{\pi}, \epsilon R[h,T])$, where the function $\epsilon R(h,T)$ would be the "reaction" force of the ROM variables on the MJO/WWB system. However, for sake of simplicity we shall consider hereafter $\epsilon R(h,T) = 0$ as in B_16. The feedback term can be included following the more general approach of Refs. 22 and 23.

Suitable values of ω and λ (the "friction" coefficient) can be obtained via phenomenological considerations when deriving the ROM from building block equations,[4,5] and/or directly from a fit to observations.[28] Realistic ranges are $2\pi/48$ months$^{-1} \le \omega \le 2\pi/36$ months^{-1} and $1/12$ months$^{-1} \le \lambda \le 1/6$ months^{-1}.

If we substituted the booster variable ξ with white noise in Eq. (1), we would obtain a Stochastic Differential Equation (SDE) with correlated additive and multiplicative (CAM) white noise. In the recent geophysics literature, one dimensional SDEs with white CAM noise have been extensively studied and used to model large-scale atmospheric and oceanic variables interacting with fast fluctuating forces.[36–40] The introduction of white noise to mimic the dynamics of fast chaotic perturbing forces, reducing the deterministic

dynamics to a Markov stochastic process is, of course, very common in statistical mechanics. This procedure has been formally justified by old well-known works about limit theorems (e.g., Ref. 41) and also by more recent ones, introducing some specific chaotic hypothesis (e.g., Refs. 42 and 43). Actually, the mathematical theorems proved were for mechanically very special mathematical model systems, like very chaotic systems which, from a physical point of view, looked often highly idealized to be relevant for physics. In any case, once assumed to work in a stochastic framework, well known classical theorems help us to generalize this result, showing that a very broad class of stochastic dynamical systems converge (in a weak sense) to diffusion Markov processes.[44] More recent works have formally shown that, in some special cases, also a process with a finite correlation time can be reduced to a Markov stochastic process by dividing the dynamics into Markov partitions (for a review, see, e.g., the book of Dorfman[45]).

In practical cases, however, it is often not possible to prove that the system we are interested in satisfies all the hypothesis requested by the theorems that allow the formal link between dynamical deterministic systems and stochastic processes. For example, when the stochastic perturbation has a multiplicative character and/or the perturbed system is nonlinear, it is not formally clear how to proceed to obtain this Markov partition. Actually, it is obvious that this reduction to a simple Markov process of non-linear dynamical systems perturbed by stochastic colored noise is not in general possible. In any case, these approaches aim at describing the statistics of the interested process by an affective Markov process. The corresponding FPE is thus a parabolic Partial Differential Equation (PDE)[46] where the transport coefficients are given by standard Green-Kubo relations[47] like the classical Einstein formula for the diffusion coefficient of the Brownian motion:

$$D \sim \int_0^\infty dt \langle f(0) f(t) \rangle .$$

This formula, that relies on the validity of the central limit theorem, either in its original strict version or in the more general recent weak version, does not hold true, of course, if the system of interest is not linear and/or if the perturbation $f(t)$ depends on the variables of interest.

In conclusion, using a simple CAM noise to force the slow dynamics of the ROM leads to some issues:

- the dynamics of the oceanic variables (h and T) and that of the atmosphere variables (MJO/WWB) have time scales that are not separated enough to justify "a priori" the white noise approximation for the ROM perturbation. The nonlinear nature of the coupling between the slow dynamics of the ROM and of the perturbation does not allow to safely use the standard procedure of dividing the correlated dynamics into Markov partitions;
- if we try to go beyond the white noise approximation we will have to take into account the well known fact that in principle the Kramers-Moyal expansion of the master equation does not allow momentum truncations beyond the second order and/or decorrelation hypothesis, so that we cannot obtain a FPE for the PDF of the ROM variables;
- it follows from the previous points that in the stochastic framework, the role of the separation of time scales is difficult to be controlled, therefore, in the same framework the justification of white noise approximation for stochastic perturbations with finite time scale is subjected to well founded criticisms.
- in the presence of multiplicative noise (i.e., noise whose intensity depends upon a function g of the system's state, here $g = 1 + \beta T$), we face the well-known Itô-Stratonovich dilemma, i.e., we have to choice a consistent interpretation and calculation scheme of the noise structure. In the Itô approach, the choice is so that the Martingale property of the stochastic process is preserved in time. In contrast, the Stratonovich approach abandons the Martingale property but obeys the normal rules of calculus and leads to a modified drift term when compared to the Ito case.

For example, Jin *et al.*[18] consider the case where ξ is a red noise process, and they need to use an "*ad hoc*" stochastic closure hypothesis to truncate the chain of the differential equations of moments.

In B_16 and here, on the contrary, we consider the forcing $\xi(t)$ as part of a generic *deterministic* system, and use a perturbation-projection approach borrowed from works on foundation of Thermodynamics and Statistical Mechanics[30,48–50] (adapted to non-Hamiltonian systems[20,21]) to project out the explicit dynamics of the booster. Using this approach, we directly obtain a FPE for the PDF of the ROM variables without the need of assuming a very large separation between the timescales of the unperturbed ROM and the booster. The link with the SDE is "*a posteriori*" because the FPE can, in turn, be related to an equivalent stochastic process.

Using this projection perturbation approach, the FPE is obtained by retaining only the lowest non-zero order in the parameter coupling the system of interest and the booster (MJO/WWB, etc.) of the whole system. Therefore, it is clear that in principle all the higher order terms are *not* vanishing as in the stochastic case, but we can control and limit the contribution of the non-Fokker Planck terms by restricting the allowed values of the coupling parameter. This is exactly the same procedure adopted in Quantum Mechanics perturbation theory. We stress that although the equation of motion of the whole deterministic system is Markovian (the trajectories are fully determined by the initial conditions), the projection approach makes the dynamics of the system of interest non-Markovian. The Markovian-like character of the statistics of the system of interest is recovered as a limiting case only after the assumption of a finite correlation time τ of the booster variable ξ and the assumption that *we are interested in the large time scale dynamics of the relevant part* (the ROM variables). We will see that being a Markovian approximation of an intrinsically non-Markovian process, the FPE we obtain with this dynamical approach is a hyperbolic PDE,[51] rather than parabolic as for a pure Markovian stochastic process.

B_16 used the FPE obtained to determine the stationary PDF and the first moments of the perturbed ROM. Here, we focus on the average recurring times of ENSO events.

In Appendix A 1, we report a short summary of the projection procedure, adapted to the present case, as described by Eqs. (1) and (2). Hereafter, we give only the result, but we think worthwhile stressing again that respect to other standard cases (as in chemical reaction theories[50] or as in works about foundation of thermodynamics[30]), where the projection approach is applied to Hamiltonian systems, or at least where the system of interest is Hamiltonian (o reducible to an Hamiltonian structure increasing the number of degrees of freedom) and the interaction with the booster variable is Hamiltonian (namely, it is the gradient of some potential), in the present case, neither the ROM neither the interaction with the booster are compatible with an Hamiltonian structure. This is because the ROM is dissipative and because the perturbation depends on the T variable (that plays the role of the velocity if we consider the ROM as a standard linear oscillator). In Refs. 21–23, it has been shown that for Hamiltonian systems of interest the energy conserving property (or the Poisson brackets formalism) of the time evolution simplifies a lot the projection procedure. In non-Hamiltonian cases, energy conserving and Poisson brackets formalism cannot be used and we must rely in the more general formal framework of the Lie algebra to solve the calculus with the Liouville operators involved by the perturbation projection approach (see Ref. 52).

That specified, for weak perturbation (lowest non-vanishing order in ϵ), we obtain the following FPE for the reduced PDF $\sigma(h,T;t)$ of the ROM (hereafter $\partial_t \equiv \partial/\partial t$, $\partial_h \equiv \partial/\partial h$, and $\partial_T \equiv \partial/\partial T$):

$$\begin{aligned}\partial_t \sigma(h,T;t) = \big\{&\omega\,\partial_h T - \omega\,\partial_T h \\ &+ (\lambda + D\,\beta^2)\,\partial_T T + D\,\beta\,\partial_T \\ &+ \partial_T A(h,T)\,\partial_T + \partial_T B(h,T)\,\partial_h\big\}\sigma(h,T;t),\end{aligned} \tag{3}$$

where $D \equiv \epsilon^2 \langle \xi^2 \rangle_b \tau$ is the "standard" diffusion coefficient, and the brackets $\langle \dots \rangle_b$ indicate the average over the unperturbed fast booster variable ξ, using the booster stationary PDF as weight, or the time average for ergodic dynamical systems. τ is the decay time of the auto-correlation function of ξ, i.e., if $\varphi(t) \equiv \langle \xi(t)\,\xi(0)\rangle_b / \langle \xi^2 \rangle_b$ is the normalized autocorrelation function of ξ, $\tau \equiv \int_0^\infty \varphi(t) \mathrm{d}t$.

As in B_16, the diffusion functions $A(h,T)$ and $B(h,T)$ are second order polynomials of the ROM variables (h,T) (see also Appendix A 2)

$$\begin{aligned}A(h,T) &= A_0 + \beta A_1\, h + \beta A_2\, T \\ &\quad + \beta^2 A_3\, hT + \beta^2 A_4\, T^2, \\ B(h,T) &= B_0 + \beta B_1\, h + \beta B_2\, T \\ &\quad + \beta^2 B_3\, hT + \beta^2 B_4\, T^2.\end{aligned} \tag{4}$$

The A_i and B_i coefficients are proportional to ϵ^2, they do not depend on the β parameter and they are linear combinations of the Fourier transform of the booster autocorrelation function $\varphi(t)$, evaluated at the frequencies 2Ω and $\Omega - i\lambda/2$, where $\Omega \equiv \sqrt{\omega^2 - \lambda^2/4}$ is the effective frequency of the unperturbed ROM (see Appendix A 2 for details). We obtain the result that, despite the possible complex nature of the forcing model described by the generic functions $F(\xi,\boldsymbol{\pi})$ and $\boldsymbol{Q}(\xi,\boldsymbol{\pi})$ of Eq. (2), the transport coefficients of the FPE are controlled solely by the autocorrelation function of the collective complex forcing ξ and by the multiplicative character of the interaction with T (represented by the β parameter).

The implication of this result is that we would obtain the same FPE by replacing the complex deterministic forcing with just a noise term, provided that the autocorrelation function of the noise is the same as that of ξ. For example, if we assumed that the normalized autocorrelation function $\varphi(t)$ decays exponentially, i.e., $\varphi(t) = \exp(-t/\tau)$, we would obtain a deterministic and general derivation of the ROM driven by the red noise of Refs. 18 and 19. For a linear interaction (i.e., $\beta = 0$), the diffusion coefficients do not depend on the state of the ROM, and we would obtain a standard diffusion process. Thus, using the projection perturbation approach to the ROM, we obtain a result that on one hand agrees with well-known works about stochastic processes (e.g., Ref. 44), but on the another hand, in spite of the less mathematical robustness and rigor with respect to the classical formal results, gives us directly the specific FPE, without constraints like the time scale separations (or similar ones), for the PDF of our deterministic linear/nonlinear systems, and under very weak assumptions.

The presence of the coefficient B is an indication of the non-Markovian nature of the booster. If $\xi(t)$ were a Markovian process (white noise) it would have a vanishing decay time of the autocorrelation function, and in this case B vanishes too, as it can be seen from its explicit expression given in Appendix A 2.

We emphasize again that from the FPE it is possible to obtain all the important statistical features of the ROM. For example, it is remarkable that for the present case, where we have a CAM forcing, as shown in B_16 and also reported in Appendix A 3, it is straightforward to get the *exact and closed* equation of motion for any order of the moments of the variables (h,T). In Appendix A 3, we obtain explicitly the equation of motion of the first two moments (the mean of h and T and their variance), and we see that the dynamics of the h and T averages (and thus, that of the "lag t" auto and cross correlation functions) is the same as that of a linear damped oscillator with a constant forcing and additive white noise. Obviously, this "effective" linear oscillator does not have the same coefficients of the bare ROM: frequency and relaxation time are modified by the multiplicative interaction with the booster.

It is worth stressing that for weak perturbations (small ϵ values) the spread of the T variable, namely, $\langle T^2 \rangle_s$ (hereafter the subscript s stands for *stationary*), depends only weakly on the β parameter (but the skewness and the Kurtosis *strongly depend on* β). In fact, the spread of the T variable can be written as (see Appendix A 2)

$$\begin{aligned}\langle T^2 \rangle_s &= \frac{A_0}{\lambda - 2\,\beta^2 A_4}\left(1 - \frac{\beta^2 A_3}{\beta^2 A_3 + \omega}\right) \\ &\approx \frac{A_0}{\lambda}\left[1 + \beta^2\left(2\frac{A_0}{\lambda} - \frac{A_3}{\omega}\right)\right] + O(\epsilon^6) \approx \frac{A_0}{\lambda} + O(\epsilon^4).\end{aligned} \tag{5}$$

In Eq. (5), the approximate expression in the second line relies on the linear dependence of the coefficients A_i on ϵ^2 (see Appendix A 2). The approximate expression for $\langle T^2 \rangle_s$ shown in Eq. (5) implies that the width of the reduced PDF of the T variable is always close to the width of the Gaussian distribution we obtain for $\beta = 0$. This fact will be used in Sec. III.

A crucial aspect of the results is that the dynamics of the first two moments depend only weakly on the time scale separation between the unperturbed ROM and the forcing booster. This important fact is *derived* analyzing the exact equations of motion of the moments (see again Appendix A 3) and it is not just *assumed a priori* as usually done when using white noise. Thus, we can simplify the FPE of Eqs. (3) and (4) by safely taking, *a posteriori*, the limit of very large time scale separation between the dynamics of the ROM and that of the fast booster (first order in τ in the limit $\tau\omega \to 0$, $\tau\lambda \to 0$). As a result, we have $A_1 = A_3 \sim 0$, $A_0 \sim A_2/2 \sim A_4 \sim D \equiv \epsilon^2 \langle \xi^2 \rangle_b \tau$, $B \sim 0$ (see Appendix A 4), so that the diffusion coefficients of the FPE become

$$\begin{aligned} A(T) &= D\,(1+\beta T)^2 + O(\tau^2), \\ B(T) &= 0 + O(\tau^2), \end{aligned} \tag{6}$$

leading to the following FPE from Eq. (3)

$$\begin{aligned} \partial_t \sigma(h,T;t) &= \big\{\omega\,\partial_h T - \omega\,\partial_T h + \lambda\,T + D\,\beta\partial_T(1+\beta\,T) \\ &\quad + \partial_T D\,(1+\beta T)^2 \partial_T\big\}\sigma(h,T;t), \\ &= \big\{\omega\,\partial_h T - \omega\,\partial_T h + \lambda\,T - D\,\beta\partial_T(1+\beta\,T) \\ &\quad + \partial_T^2 D\,(1+\beta T)^2\big\}\sigma(h,T;t). \end{aligned} \tag{7}$$

In a nutshell, the time scale separation is not as critical as the value of the multiplicative coupling parameter β, if we are interested in the dynamics of the first moments of the ROM. However, when the timing of rare events is concerned, this may no longer be the case. In fact, from the general FPE of Eq. (3), obtained by the projection approach, we see that a finite time scale separation between the ROM and the fast forcing results in a non-vanishing cross diffusion term $\partial_T B(h,T)\partial_h$ in the FPE. This term breaks the parabolic structure of the simplified FPE of Eq. (7) and it increases the effective dimensionality of the system; and in turn this could affect the dynamics of rare events in a non-negligible way. Nevertheless, we will still use the simplified FPE of Eq. (7) to get the analytic expression for the average timing for ENSO events. This is so because we are not interested in a precise estimate of the average recurring times of El Niño events, but in evaluating the influence of the non-Gaussian structure of the stationary FPE on the recurring times.

The FPE of Eq. (7) allow us to make a link with a SDE picture of the perturbed ROM. In fact, the structure of this FPE, and, in particular, the "noise-induced drift" term $-D\,\beta\partial_T(1+\beta\,T)$ of the last equality of Eq. (7), suggests we can consider Eq. (1) as a SDE with the Stratonovich interpretation for integration.

III. THE STATIONARY PDF

We stated above that from the FPE, taking advantage of the well-tested procedures used to recover thermodynamics from microscopic dynamics, we can get important information about the statistics of the system. However, the FPE in Eq. (7), due to the multiplicative character of the forcing, that depends on the T variable (which plays the role of the velocity if we considered the ROM as a linear dissipative oscillator), has not an Hamiltonian origin. So that its stationary solution is neither Gaussian nor Canonical {e.g., $\propto \exp[-H(h,T)/\Theta]$, where $H(h,T)$ is some Hamiltonian function and Θ is some parameter). Still, it is possible, using a reasonable ansatz, to obtain the following analytic expression for the stationary PDF of the T variable (see Appendix B)

$$\begin{aligned} p_s(T) &= \beta f_\mu\left(\frac{\mu-2}{1+\beta T}\right) \quad \text{for } T > -1/\beta, \\ p_s(T) &= 0 \quad \text{for } T \le -1/\beta, \\ \mu &\equiv 1 + \frac{\lambda}{D\beta^2}, \end{aligned} \tag{8}$$

$$\mu \equiv 1 + \frac{\lambda}{D\beta^2}, \tag{9}$$

where the Gamma-like density function $f_\mu(x)$ is defined as

$$f_\mu(x) \equiv \frac{1}{(\mu-2)\Gamma(\mu-1)} e^{-x} x^\mu, \tag{10}$$

in which $\Gamma(a)$ is the standard complete Gamma function. The dimensionless parameter μ must be greater than 3 to have both a finite normalization of the reduced PDF and the existence of (at least) the first two moments. This stationary PDF depends only on the value of the β parameter that controls the relative intensity of the multiplicative part of the perturbation, and on the ratio of the diffusion (D) and frictional (λ) coefficients (the "temperature" parameter in the corresponding Brownian motion picture, where T is the velocity of the Brownian particle and the booster represents the thermal bath) via the μ parameter of Eq. (9). The values of D/λ can be obtained from observations with a reasonable accuracy. In fact, according to the exact relationship of Eq. (5), to the second order in ϵ the variance of this PDF is well approximated by $A_0/\lambda \sim D/\lambda$, namely, it is independent of β. Thus, D/λ can be inferred from the variance σ^2 of the Niño3 time series, leading to values of D/λ of about 0.8.

It is easy to check analytically that in the limit $\beta \to 0$ and D/λ fixed, the stationary PDF in Eqs. (8)–(10) becomes a standard Gaussian with the same variance D/λ. However, for $\beta \neq 0$, the stationary PDF is clearly non-Gaussian. In fact, for large positive T it has a "power law" tail that makes possible high fluctuations of positive values of T (strong El Niño events). From Eq. (9), we have that the μ parameter, which controls the decay of this "heavy" tail of the stationary PDF, strongly depends on the value of the β parameter. Although the average value of T is close to zero, the maximum of the stationary PDF is found at $T_{max} = -2/(\beta\mu) \approx -2\beta\,D/\lambda$, namely, for fixed D/λ, it is proportional to β. Notice also that for negative values of T (La Niña events) the probability of strong events is largely reduced and it has a threshold

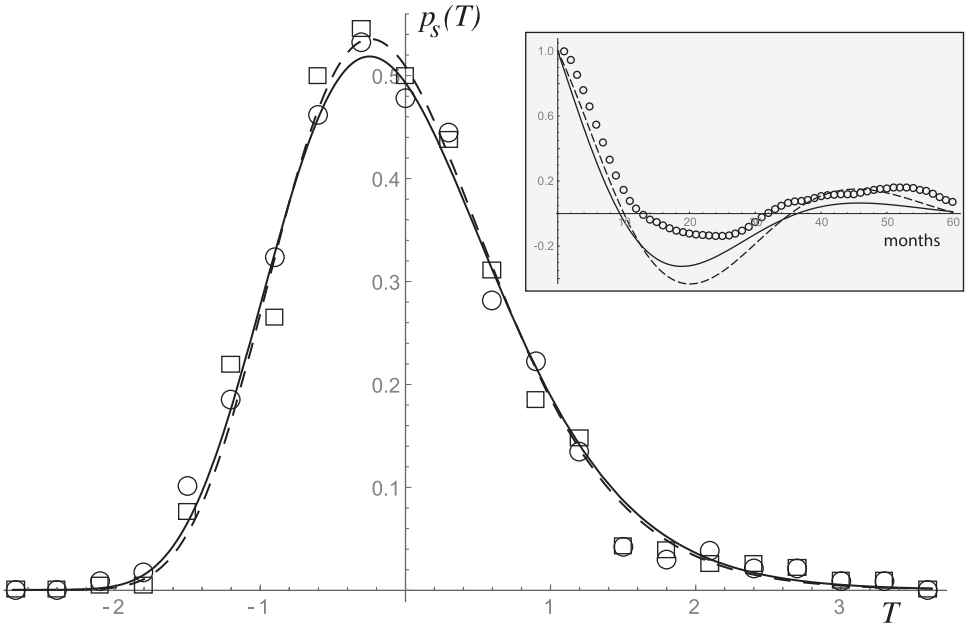

FIG. 1. Best fit of the stationary PDF of Eqs. (8)–(10) (solid line) with the normalized frequency of the one month (circles) and three months (squares) average Niño3 data from NOAA (http://www.cpc.ncep.noaa.gov/data/indices/). From the fit, we get $\beta = 0.19$ and $\mu = 34$. Dashed line and squares: the same as the solid line and the circles, respectively, but with a three months average of the data. In this case, we get $\beta = 0.21$ and $\mu = 31.4$. In the text, we use the values $\beta = 0.2$ and $\mu = 32.7$. Inset: normalized autocorrelation function of T. Circles: from the NOAA Niño3 data. Solid line: from the FPE of Eq. (7) with $\lambda = 1/6$ months^{-1}. Dashed line: as the previous but with $\lambda = 1/12$ months^{-1}.

at $T_{min} = -1/\beta$. It is apparent that these non-Gaussian features are shared by the Niño3 data, as seen by Fig. 1. The agreement with the observed PDF of the Niño3 index was also shown by B_16 using $\beta = 0.2$ and $D/\lambda = 0.66$. Here, we use an improved fitting approach by constraining $D/\lambda \sim 0.8$ and obtain $\beta = 0.2$, leading to $\mu = 32.7$.

While the value of the quantity D/λ can be determined reasonably reliably as the variance of the data (thus it may be considered as well-established and fixed), the value of the β parameter depends on "finer" features of the statistics of the data, such as the tails of the PDF, where the number of available data is small. For fixed D/λ, the parameter μ [Eq. (9)] depends only on β, and the stationary PDF itself can be considered as controlled uniquely by β. In Fig. 2, we show the stationary PDF of Eq. (8) for $\beta = 0.2$ and for $\beta \to 0$ (corresponding to a Gaussian function). In Sec. IV, we will explore the dependence of the recurrence time of El Niño events on β.

As anticipated in Sec. II, the value for the relaxation parameter λ of Eq. (1) has been obtained in the literature by using phenomenological considerations when deriving the ROM from building block equations,[4,5] and/or directly from a fit to observations.[28] The estimates range from $1/12$ months^{-1} to $1/6$ months^{-1}. However, the value of λ could also be obtained, in principle, by comparing the autocorrelation functions of the T variable obtained from observations with that obtained from the FPE of Eq. (7). The expression for the latter is $\langle T(t)T(0)\rangle_s/\langle T^2\rangle_s = e^{-\Gamma t/2}\,(\cos[\Omega t] - \Gamma \sin[\Omega T]/\Omega)$, with $\Omega \equiv \sqrt{\omega^2 - \Gamma^2/4}$ and $\Gamma \equiv \left(\lambda - D\beta^2\right)$. The theoretical autocorrelation function from the above expression for $\lambda = 1/6$ months^{-1} and $\lambda = 1/12$ months^{-1} are compared with the autocorrelation function of the observed Niño3 index in the inset of Fig. 1. Clearly, even with this approach, uncertainties remain. We shall see that the comparison of the timing of El Niño events obtained analytically from the ROM with

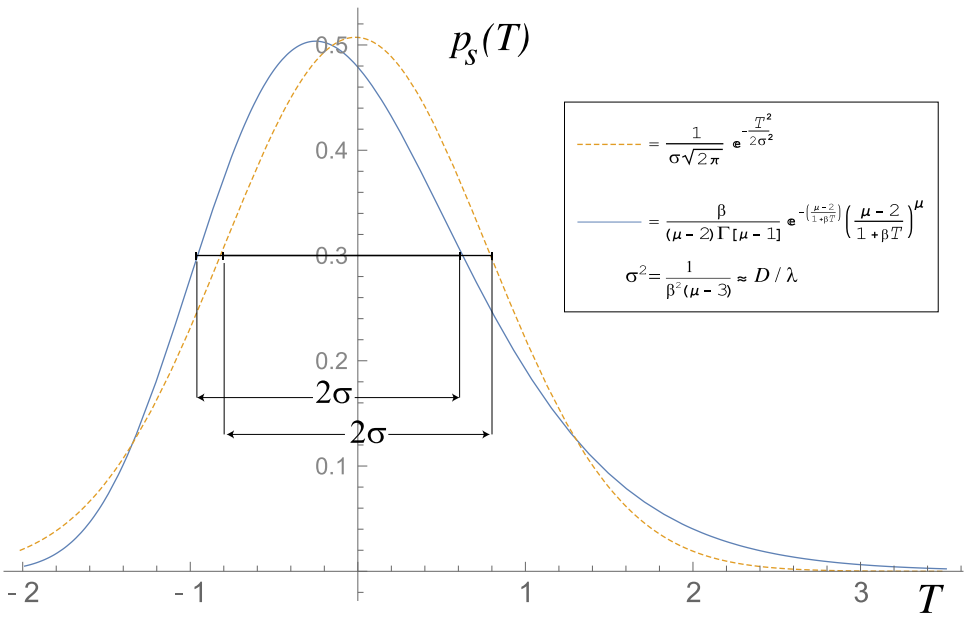

FIG. 2. Solid line: the stationary PDF of Eqs. (8)–(10) with $\beta = 0.2$ and $\mu = 32.7$. Dashed line: the Gaussian function with the same variance of the stationary PDF, corresponding to Eqs. (8)–(10) in the limit $\beta \to 0$ and D/λ fixed.

the observed average timing of weak and intermediate ENSO events (for which the statistics is significant) will constrain the possible range of values for the friction coefficient of the ROM.

IV. THE MEAN FPT FOR ENSO EVENTS

As already stressed, the main focus of the present paper is to use the model described by Eqs. (1) and (2) to estimate the average time we have to wait for the onset of a "strong" El Niño event, starting from a "neutral" initial state. The latter is defined as the case where the initial temperature T_i has a value in the range $-0.5 \leq T_i \leq 0.5$. As depicted in Fig. 3, "strong" El Niño events are identified with the criterion $T > 1.5$. The stationary PDF that we use for the T variable is given in Eqs. (8)–(10). Notice that for an ergodic system (which is an obvious implicit assumption in the present approach) the stationary PDF, evaluated at a given target temperature T_{tg}, $p_s(T_{tg})$ provides directly the average rate at which a very long trajectory of the system passes through the given target value T_{tg}. The average period between passages can then be obtained as $2/p_s(T_{tg})$ (the factor 2 is used because the long trajectory, after going through the target value T_{tg} from below, it will always pass the same target value from above, coming back to lower values of T, "counting" twice the same event). However, $2/p_s(T_{tg})$ is not exactly the information we are interested in. In fact, after reaching the target value T_{tg}, the trajectory may continue to fluctuate around it, thus increasing the average rate. What we are really interested in is a mean *First Passage Time* (FPT), which deeply involves the dynamical features of the statistics, and which, in turn, relates to the full FPE of Eq. (7), rather than the sole stationary PDF.

The study of the FPT problem started more than a century ago, but its diverse applications in science and engineering mostly emerged in the last two to three decades. Assuming that $T(t)$ is a one-dimensional stochastic process, the FPT is defined as the time $\delta t(T_i \mid T_{tg})$ when $T(t)$ first crosses a given target T_{tg}, starting from the initial value T_i (see Fig. 4). But, if $T(t)$ is a stochastic process, repeating many times the same "experiment" should lead to different values for $\delta t(T_i \mid T_{tg})$, so that the FPT itself is a stochastic process, with its own PDF. We indicate with $t_n(T_i \mid T_{tg})$ the n-th moment of the PDF of the FPT. Thus, the mean FPT is given by $t_1(T_i \mid T_{tg})$.

In our model of Eqs. (1) and (2), the fluctuations of the ENSO variables (h, T) stem from the *weak* interaction of the ROM with the fast perturbation $\xi(t)$, thus, we expect that typically, for small values of the target temperature anomaly (e.g., $T_{tg} < 1$), the time scale of the FPT is governed by the unperturbed ROM dynamics, namely, a few years. On the opposite, for very large target values (e.g., $T_{tg} > 3.5$), we can expect that the positive feedback mechanism (the multiplicative part of the perturbation) must dominate, and that happens only when we have an unlikely sequence of positive values of the fast forcing. Thus, these strong spikes, embedded in a background of many minor fluctuations, are fast, rare, and uncorrelated with each other, namely, they are Poisson-like random events that decay quickly with a timescale of the order of $1/\lambda$. In this case, the average period between two consecutive events is well approximated by the double of the inverse of the stationary PDF.

In between these two extremes, the mean FPT cannot be estimated so easily, and must be obtained by working with the FPE of Eq. (7).

In principle, First Passage Time (FPT) techniques[53–56] can be applied to any kind of FPE, and allow one to obtain a closed recursion formula for the moments of the PDF of the FPT, which involves the stationary PDF and the transport coefficients of the FPE.[57,58] However, as also emphasized in B_16, we cannot even find an exact analytic expression for the stationary PDF of the two-dimensional FPE of Eq. (7), thus we use the already cited ansatz to reduce the dimensionality of the system to one, and to obtain the approximate reduced stationary PDF given in Eq. (8). An important issue is, of course, the legitimacy of using this ansatz for evaluating the FPT of strong events. In Appendix C 1, it is shown that if the ansatz introduced in B_16 gives the exact reduced stationary PDF for the T variable, then the same *ansatz* can be legitimately used in the calculation of the moments of the FPT. The *ansatz* allows us to obtain a good approximation of the stationary PDF. Unfortunately, the FPT for strong events is sensitive to the details of the tails of the stationary PDF, details that may not be well reproduced by the approximate analytical expression of Eq. (8) obtained exploiting the ansatz. This ansatz corresponds to a "crude" reduction of the dimensionality of the system of interest from the initial two degrees of freedom (h, T) to only one (T), and a path in the two dimensional space (h, T) takes, in general, more time than a path

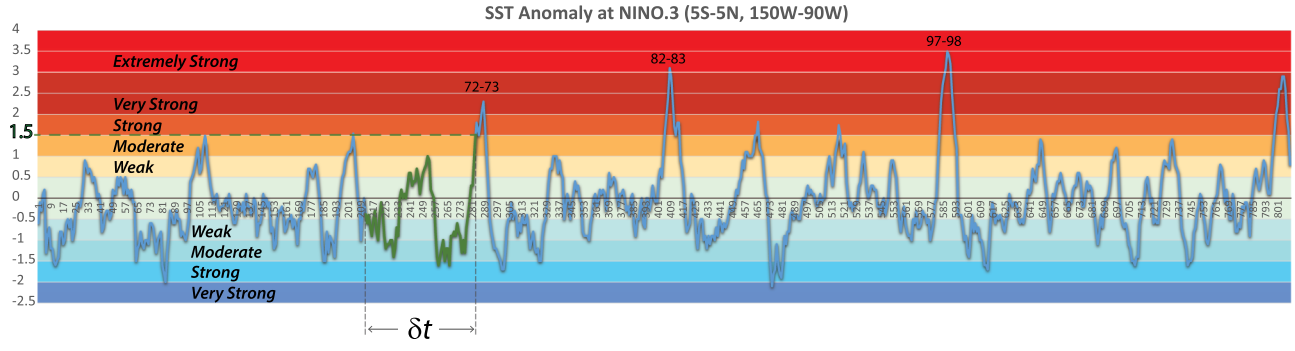

FIG. 3. The month average Niño3 index from January 1949 to February 2016. Data from the Tokyo Climate Center, WMO Regional Climate Centers (RCCs), http://ds.data.jma.go.jp/tcc/tcc/. In green color, one of the path for the First Passage Time (FPT) $\delta t(T_i, T_{tg})$ for a given target temperature anomaly T_{tg} (here $T_{tg} = 1.5$), starting from an initial temperature T_i [$-0.5 \leq T_i \leq 0.5$, see also the text and Fig. 4 for details about the FPT].

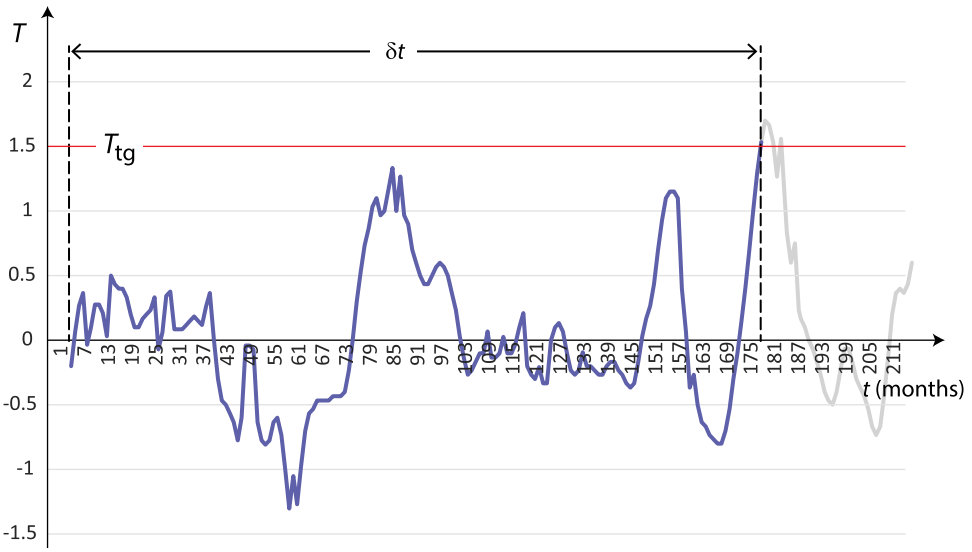

FIG. 4. The First Passage Time $\delta t(T_i, T_{tg})$ for a target temperature anomaly of $T_{tg} = 1.5$ is defined as the first time the fluctuating temperature $T(t)$ cross the threshold T_{tg} (1.5 in this case), starting from an initial temperature T_i (that we will choose in the range $-0.5 \leq T_i \leq 0.5$).

in a one dimensional space (T), to reach a given threshold in the T axis. However, even with these caveats, we shall continue to use the same ansatz also for the calculation of the FPT. This will allow us to obtain an analytical result that can contribute to shed some light on the role played by the multiplicative noise and by the relaxation time of the ROM in affecting the average timing of strong ENSO events. We need to keep in mind, however, that the average timing that we obtain with this approach must be considered as a reasonable "round down" approximation for the true FPT of the ENSO.

Using standard results of the FPT literature[57,58] (see also Appendix C 1), we have

$$t_1(T_i \mid T_{tg}) = \int_{T_i}^{T_{tg}} \frac{\mathrm{d}T}{A(T)\, p_s(T)} \int_{-\frac{1}{\beta}}^{T} p_s(T')\mathrm{d}T', \tag{11}$$

$$t_2(T_i \mid T_{tg}) = \int_{T_i}^{T_{tg}} \frac{\mathrm{d}T}{A(T)\, p_s(T)} \int_{-\frac{1}{\beta}}^{T} p_s(T')\, t_1(T' \mid T_{tg})\mathrm{d}T'. \tag{12}$$

The above two equations show explicitly that the moments of the PDF of the FPT depend not only on the stationary PDF of the FPE but also on the diffusion coefficient $A(T)$. Using Eq. (6), we have $A(T) = D\,(1+\beta T)^2 = \lambda\,\sigma^2\,(1+\beta T)^2$, where $\sigma^2 = 0.8$ and $\beta = 0.2$, as discussed in Sec. III. Inserting this expression for $A(T)$ in Eq. (11), it results that the average FPT depends inversely on λ. As discussed in Sec. III, reasonable values for λ should be in the range $1/12$ months$^{-1} \leq \lambda \leq 1/6$ months^{-1}.

Substituting the stationary PDF of Eqs. (8)–(10) in Eqs. (11) and (12), we can easily numerically determine the values of the first two moments of the FPT for different values of λ. However, with a little algebra and some minor approximations, from Eq. (11), we can also get the following analytical result (see Appendix C 2 for details)

$$t_1(T_i \mid T_{tg}) = \left\{ \frac{2}{p_s(T)} \times \frac{\beta}{2\lambda} \frac{M\left[1, -(\mu-2), -\frac{\mu-2}{\beta T+1}\right]}{\beta T+1} \right\}_{T_i}^{T_{tg}}, \tag{13}$$

where, for any function $g(x)$, we define $\{g(x)\}_a^b \equiv g(b) - g(a)$, and $M\,[1, y, z]$ is the Kummers (generalized hypergeometric) function of the first kind with first argument equal to one. The analytical result of Eq. (13) gives much more physical information about the mean FPT for the ENSO model of Eqs. (1) and (2) than just numerical simulations. In fact, the first factor term inside the curly brackets in the r.h.s. of Eq. (13) is twice the inverse of the stationary PDF, which, as we have previously noticed, should be a good approximation for the mean FPT when events can be considered uncorrelated with each other. The second factor term is the correction to this approximation and it is proportional to the Kummers function. We can see in Fig. 5 that for $\lambda \sim 1/6$, the correction factor is close to unity for $T \sim 3.5$. On the other hand, this is not the case for $\lambda \sim 1/12$, indicating that for the smaller values of λ, some correlations remain also among the rare largest events. We stress that this finding agrees with the work of Wittenberg[59] that analyzed the data from 2000 years run of global coupled GCM. It is also interesting to note that for the present μ and β parameters and in the range of realistic T values, the Kummers function in Eq. (13) does not have any simple behavior nor it can be approximated by some simple limit function.

Using Eq. (13) we show, in Fig. 6, the dependence of the mean FPT on T_{tg} for different values of the λ parameter, compared with the mean FPT obtained from observations (circles).

From this figure, we see that $\lambda = 1/12$ months^{-1}, i.e., a value at the lower end of the allowed λ range, provides the best agreement between observational estimates and our analytic result for the mean FPT. In fact, with $\lambda = 1/12$ months^{-1}, the mean FPT for intermediate target temperatures, obtained from Eqs. (11) or (13), is in the range 2–7 years, in good agreement with the observed intervals between intermediate El Niño events. The increase in FPT with decreasing λ for a fixed T_{tg} may seem at first counterintuitive. In fact, for a given diffusion coefficient D (i.e., for a constant intensity of the booster variable ξ, recall that $D = \epsilon^2 \langle \xi^2 \rangle_b \tau$) *decreasing* the "friction" parameter λ would *increase* the width of the stationary PDF. This, in turn, would *decrease* the average

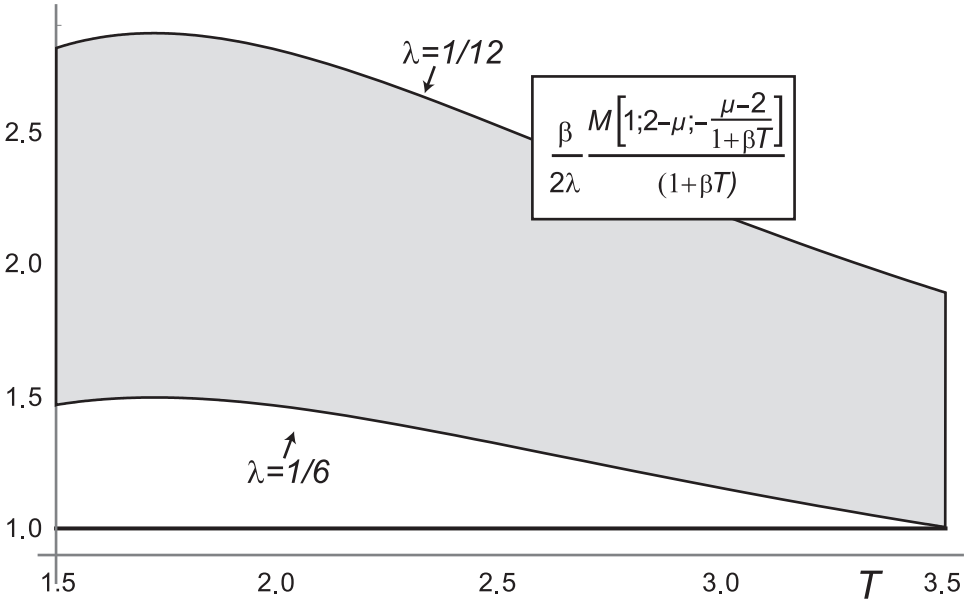

FIG. 5. The correction factor term in the analytical expression for the mean FPT given in Eq. (13) for λ in the range 1/12 months^{-1} ≤ λ ≤ 1/6 months^{-1} (see the text for details).

FPT for any T_{tg} since the probability to have high T values would also increase. However, this is not our case because the observational data constrain the width of the stationary PDF, so that, instead, the resulting average FPT is *inversely* proportional to the relaxation parameter λ. From a physical point of view, this can be related to the fact that for large λ, the events are less correlated to each other.

Strong and very strong El Niño events are extreme events, and as such they are rare, so that it is not possible to have a sufficiently large observational sample size to validate our analytical results [for example, the Niño3 index from the NOAA data center (http://www.cpc.ncep.noaa.gov/data/indices) includes only 3 events with $T \geq 2.0$ and just one with $T \geq 2.75$]. Therefore, we cannot use these data to validate our analytical results, but, vice versa, we can use our analytical solution as a reasonable extrapolation of the mean FPT for these strong or very strong El Niño. The reliability of this extrapolation is based on two main observations:

- the validation of both the perturbed ROM of Eqs. (1) and (2) and the projection/FPE approach based on the analysis of the stationary PDF and of the first two moments of the Niño3 index;
- the relatively good agreement that we have found between our theoretical results and observational data for weak and intermediate El Niño events.

We think worthwhile to stress again that from the analytical expression of Eq. (13), we can evaluate how the FPT depends on the relevant parameters of the system. Apart from the inverse proportionality relationship with the relaxation coefficient λ, it is also clear that the FPT has a strong sensitivity to the value of the β parameter (notice that, once the variance $\sigma^2 = D/\lambda$ is fixed, the μ parameter depends only on β as $\sim 1/\beta^2$). In Fig. 7, we compare the average FPT obtained from the analytical expression of Eq. (13) with both observations and the values derived through the numerical integration of the stochastic differential equation equivalent to

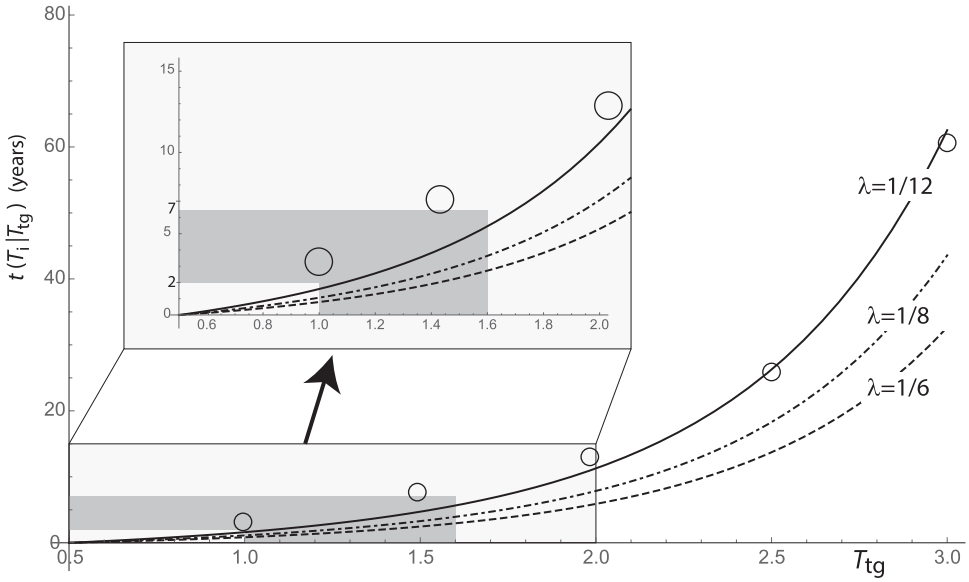

FIG. 6. The mean FPT for different values of the λ parameter, vs the target temperature, obtained using directly Eq. (13), compared with observations (circles). The values of the β and μ parameters have been fixed by the fit of the stationary PDF to the observation data: $\beta = 0.2$ and $\mu = 32.7$ (see text for details). Dashed line: λ = 1/6, dot-dashed line λ = 1/8, solid line λ = 1/12. In the inset, a zoom of the same graph, where we emphasize with a gray background the range of 2–7 years and $1.0 \leq T \leq 1.6$ corresponding to the typical recurring times interval for intermediate El Niño events. We see that the curve obtained with λ=1/12 falls better than the others in this zone.

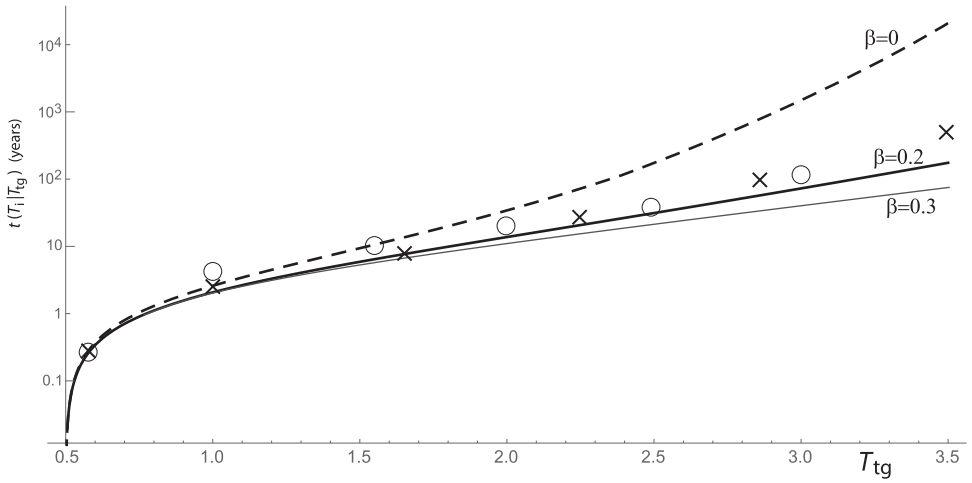

FIG. 7. Semi-log plot of the average FPT as a function of the target temperature T_{tg}, for $\lambda = 1/12\,\text{month}^{-1}$ and $\sigma^2 = D/\lambda = 0.8$ (see text for details). Thick and thin solid lines show analytical solutions from Eq. (13) with $\beta = 0.19$ and $\beta = 0.3$, respectively; while the thick dashed line is for the case $\beta = 0$, corresponding to the pure additive forcing of the ROM [in this case the stationary PDF is the Gaussian of Fig. 2]. Circles: the average FPT from observation data. Crosses: average FPT from numerical simulations of the Îto SDE corresponding to the FPE of Eq. (7):[63] $\mathrm{d}h = -\omega T\,\mathrm{d}t$; $\mathrm{d}T = (-\omega h + D\beta)\mathrm{d}t - (\lambda - D\beta^2)T\mathrm{d}t + \sqrt{D}(1+\beta T), \mathrm{d}W$, where W is a Wiener process, $\beta = 0.19$, and $\omega = 2\pi/48\,\text{month}^{-1}$.

the FPE of Eq. (7), corresponding to the case of a very large time scale separation between the ROM and the booster. The numerical solution has been obtained for the case $\beta = 0.2$. We can see that there is a good agreement between the analytical ($\beta = 0.2$) and both observations and numerical solutions, especially for values of $T_{tg} < 3.0$. In the same figure, we also show the analytical solutions of the average FPT in the case of a pure additive perturbation ($\beta = 0$, in which case the reduced stationary PDF for the T variable is Gaussian) and for $\beta = 0.3$. We see that for weak to intermediate El Niño events ($T_{tg} \leq 1.5$), the average FPT depends only weakly on β. However, the sensitivity to β clearly emerges in the case of strong and very strong events. In particular, the pure additive forcing leads to average FPT that are several orders of magnitude larger than those obtained with $\beta = 0.2$ (note the logarithmic scale in the ordinate of the graph), while in the case of $\beta = 0.3$, the FPTs are shorter at large T_{tg}. A more extensive analysis of the dependence of the average FPT on the β parameter is shown in Fig. 8. For a given T_{tg}, the FPTs become shorter with increasing β, especially for large T_{tg}, indicating a larger likelihood of stronger El Niños when the multiplicative component of the booster increases.

Now, we examine also the second moment of the PDF of the FPT. It is particularly important to do that because of the nonconstant diffusion coefficient of the FPE in Eq. (7). In fact, usually the FPT approach is used when we are looking for the timing of large and rare fluctuations, far from the equilibrium values, for example, when the system is *typically* confined to a limited region by a very high potential barrier and we are interested in the escaping rate from this zone. This is the case, for example, for the unimolecular reaction processes,[60–62] where the thermalization induced by the interaction with a thermal bath gives rise to canonical equilibrium statistics and to the famous Arrhenius law for the reaction rate. Here, on the contrary, we have a nonstandard statistics (respect to the Gaussian/Canonical one, see Fig. 2) with a power law tail of the stationary PDF, and target values T_{tg} that are not so far from the typical values of T_i. Thus, it is worthwhile to get an idea of the dispersion of the FPT with respect to the average value, namely, the standard deviation defined by $\sigma_{FPT} \equiv \sqrt{t_2(T_i \mid T_{tg}) - [t_1(T_i \mid T_{tg})]^2}$. Numerically integrating Eq. (12), we obtain the second moment of the FPT from which we obtain the standard deviation. Figure 9 shows the ratio between σ_{FPT} and mean FPT. Not surprisingly, we

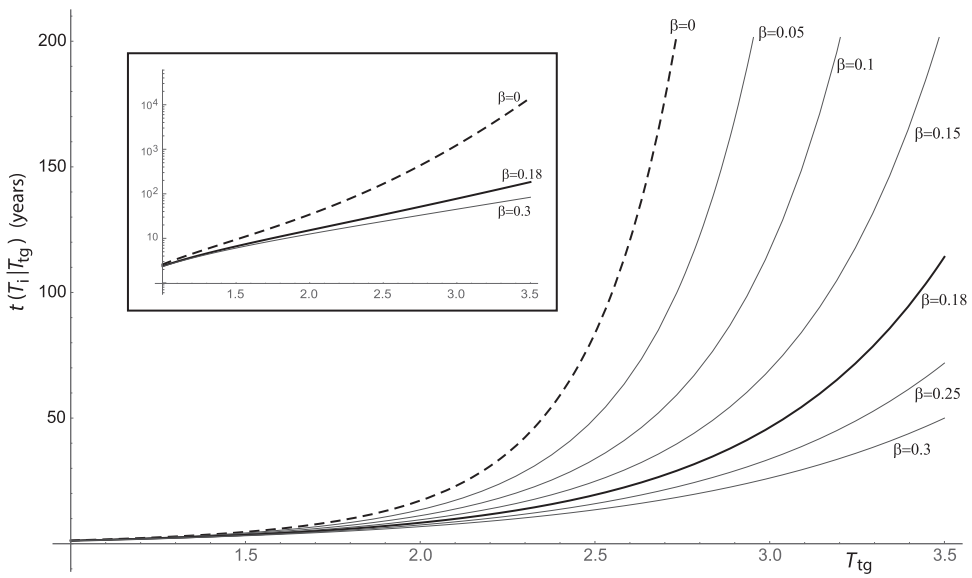

FIG. 8. Plot of the average FPT from the analytic result of Eq. (13) as a function of the target temperature T_{tg} for different values of the β parameter. In all the cases, we have set $\lambda = 1/12\,\text{month}^{-1}$ and the variance is kept fixed to 0.8 (see text for details).

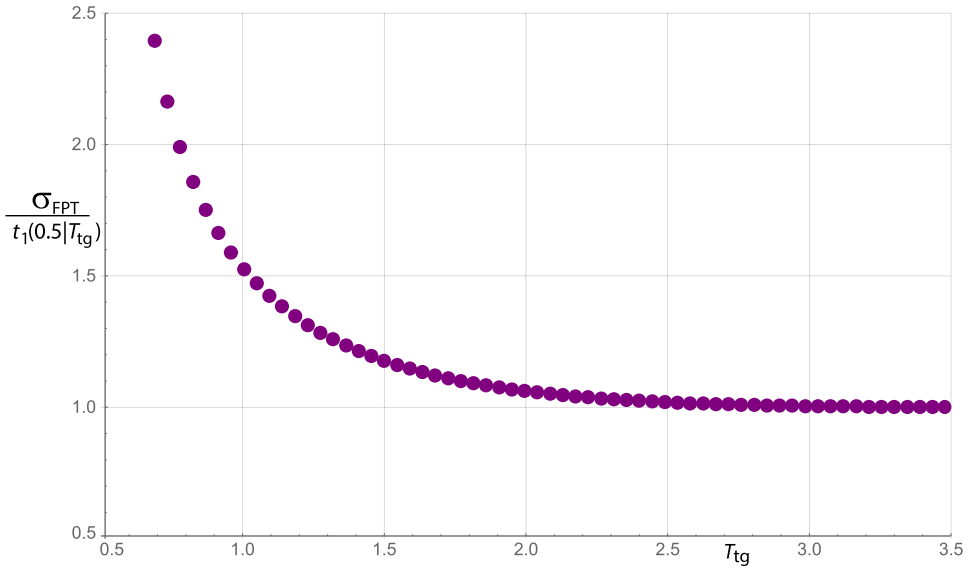

FIG. 9. The ratio between the mean FPT and the FPT standard deviation σ_{FPT} for the case $\lambda = 1/12$, where the standard deviation has been obtained by the numerical integration of Eq. (12). We can see that for weak/moderate ENSO events the dispersion of the FPT is quite large (the standard deviation is larger than the mean FPT), while for strong ENSO the dispersion decreases, and becomes very close to the mean FPT.

see that for weak El Niño events the standard deviation is larger than the average FPT, namely, the FPT has large fluctuations around the average value. However, for strong ENSO, the standard deviation becomes equal to the mean FPT. Thus, although the statistics of the perturbed ROM is not Gaussian, we can state that "the mean FPT is a good estimate of the waiting time for strong ENSO events."

V. CONCLUSION

In this paper, we build on the work of B_16 to explore other statistical aspects of the perturbed ROM, which, in spite of its simplicity, appears to provide very useful insights into the ENSO system. As in B_16, using a projection/perturbation approach, we obtain a generalized FPE for the PDF of the ROM, from which, adapting the standard FPT procedures to this nonstandard case, we get analytical expressions for the average time between strong events and for its associated standard deviation. These expressions are given in terms of transcendent Gamma and Hypergeometric Functions, a fact that is strictly connected with the "heavy" tail of the stationary PDF. The analytic solution for the mean First Passage Time (FPT) is obtained for different values of the ocean relaxation parameter λ, within a reasonable range of values for this parameter as determined through a fit to the autocorrelation function of the temperature T. We find that for $\lambda = 1/12$, we have the best agreement between the theoretical results for the mean FPT and the observed average inter-event interval (4–7 years) for intermediate ENSO events. We emphasize that the estimation of the FPTs goes beyond the information gained from the stationary PDF (already obtained in B_16) because the timing of the events deeply involves the dynamics of the statistics, and not only stationary properties (apart from the cases of unrealistically large El Niño events, e.g., $T >> 3.5$).

While confirming the suitability and usefulness of the FPE-projection approach in modeling the ENSO events developed in B_16, the present study also allows to achieve, albeit in an approximate fashion, to our knowledge the first analytical estimate of the timing of ENSO events [Eq. (13)]. From this analytical expression, we can evaluate how the FPT statistics depends on the relevant parameters of the system. For example, evaluating the behavior of the Kummer function in Eq. (13), we can quantitatively estimate the non-Poissonian features of the statistics of the ENSO events within the model studied here.

An important result that emerges from our analytical approach is that the average recurring time of very strong ENSO events is of the order of just some tens of years (about the human average life-time), with important implications for society. This result is strongly related to the multiplicative nature of the perturbation to the ROM, as expressed by the parameter β.

To test and validate these results, we have used the NOAA Niño3 index, which is based on observations covering only a limited time period, 1950 to present. To better test and validate our approach we are working on proxy data (networks of precipitation, tree-rings, corals, and ice core records) that can help extend the time series back in time some hundreds of years.[64] We believe that using these extended data, we could also take into account the dependence of the model parameters (in particular, the critical β parameter) on the global climate indexes, such as the average global temperature. Results from this approach will be presented in future studies.

In a more broad scenario, where we take into account constant or periodic forcing obtained from observed or estimated climatology, we have to improve our approach so to take into account non-autonomous (Low Order) models, either deterministic, for which we have to improve the projection method (e.g., by increasing the number of degrees of freedom to obtain an effective autonomous system), or stochastic, for which we could use the results of Ref. 69.

APPENDIX A: VERY SHORT REVIEW OF THE PROJECTION APPROACH

1. The formal approach

In the present work, we study the same dynamical systems considered in B_16, however we do not use the FPE of

Eqs. (3) and (4) in B_16 because of a marginal mistake. Equations (3) and (4) of B_16 were obtained from the results in Eqs. (54) and (55) of Ref. 21 (B_15 hereafter), using $\epsilon_1 = 0$ and making the following identification: $(x, v) \to (h, -\omega T)$, $\epsilon_0\, g'(x, v) \to \omega\epsilon G(T)$, $\Gamma \to \lambda$ and $V'(x) \to \omega^2 h$. Looking at Eq. (22) of B_15, inside the big parenthesis at the end of the second line of Eq. (22), we should find the perturbation Liouvillian operator $\partial_v g'(x, v)$ while there is the operator $g'(x, v)\partial_v$. These two operators are equal to each other only if the function g' does not depend on the v variable of the system of interest, while in the general case, we should have $\partial_v g'(x, v) = g'(x, v)\partial_v + [\partial_v g'(x, v)]$. It is the missing term $[\partial_v g'(x, v)]$ that leads to the mistake in Eqs. (54) and (55) of B_15 and, in turn, to a missing term in the FPE of Eqs. (3) and (4) of B_16.

To make the derivation self consistent, here we shortly review the Zwanzig projection approach, adapted to the present case, where the whole deterministic system (or LOM) is given in Eqs. (1) and (2), that we rewrite here

$$\begin{aligned} \dot{h} &= -\omega\, T, \\ \dot{T} &= \omega\, h - \lambda T + \epsilon\, \xi(1 + \beta T), \\ \dot{\xi} &= F\,(\xi, \boldsymbol{\pi})\,, \\ \dot{\boldsymbol{\pi}} &= \boldsymbol{Q}\,(\xi, \boldsymbol{\pi})\,. \end{aligned} \tag{A1}$$

According to the projection procedure, we divide this LOM in two parts: a part of interest, identified with the ROM variables (h, T), and the rest of the system, the booster,[21,30] represented by the variables $(\xi, \boldsymbol{\pi})$. The functions $F\,(\xi, \boldsymbol{\pi})$ and $\boldsymbol{Q}\,(\xi, \boldsymbol{\pi})$ represent the equation of motion for the booster, and they are not specified, because we do not need to know them (the booster typically will be a *nonlinear* chaotic system); however they must satisfy some specific assumptions detailed in the following. The coupling of the ROM with the booster is represented by a term that is proportional to the same booster variable ξ, namely, by the term $\epsilon\, \xi(1 + \beta T)$ in Eq. (A1). This implies some loss of generality, but not so quite as it might seem at first glance. In fact, if the "real" coupling was given by a more general function as, for example, $\epsilon f(\xi)(1 + \beta T)$, we could always redefine $f(\xi) \to \xi$ to go back to the linear form in Eq. (A1), and redefining as needed the booster equations of motion.

With respect to the more general cases in B_15, here the dynamics of the booster does not depend on the dynamics of the ROM. The dependence of the perturbing atmosphere forcing on the dynamics of the system of interest is here directly included in both the friction term $-\lambda T$ of the ROM (see the derivation of the ROM by Refs. 65 and 66) and in the multiplicative part $\beta T\xi$ of the forcing, that formally expresses the fact that the strength of part of the perturbation depends on the value of the SST anomaly.

The goal is to describe the statistics of only the part of interest, i.e., the ROM, of the LOM in Eq. (A1). From this LOM, we can write the following PDE for the PDF $\rho(h, T, \xi, \boldsymbol{\pi}; t)$ of the total system

$$\partial_t \rho(h, T, \xi, \boldsymbol{\pi}; t) = \{\mathcal{L}_a + \epsilon\, \mathcal{L}_I \xi + \mathcal{L}_b\}\, \rho(h, T, \xi, \boldsymbol{\pi}; t), \tag{A2}$$

where the unperturbed ($\mathcal{L}_a$) and perturbation ($\mathcal{L}_I$) Liouville operators, are given by

$$\begin{aligned} \mathcal{L}_a &= \omega\, \partial_h\, T - \omega\, \partial_T\, h + \lambda\, \partial_T T, \\ \mathcal{L}_I &= -\partial_T(1 + \beta\, T), \end{aligned} \tag{A3}$$

respectively. In Eq. (A2), we cannot explicitly write the Liouville operator $\mathcal{L}_b$ of the booster because it is related to the unknown functions $F\,(\xi, \boldsymbol{\pi})$ and $\boldsymbol{Q}\,(\xi, \boldsymbol{\pi})$.

We are interested in obtaining a Fokker Plank Equation (FPE) for the reduced (or marginal) PDF of the system of interest, $\sigma(h, T; t) \equiv \int \rho(h, T, \xi, \boldsymbol{\pi}; t) \mathrm{d}\xi \mathbf{d}\boldsymbol{\pi}$. Introducing the projection operator, $\mathbb{P} \cdots \equiv \wp_b(\xi, \boldsymbol{\pi}) \int \mathrm{d}\xi \mathbf{d}\boldsymbol{\pi} \cdots$, where $\wp_b$ is the stationary PDF of the booster, defined by $\wp_b(\xi, \boldsymbol{\pi}) \mid \mathcal{L}_b \wp_b(\xi, \boldsymbol{\pi}) = 0$, we have $\sigma(h, T; t) = 1/\wp_b(\xi, \boldsymbol{\pi}) \times \mathbb{P}\rho(h, T, \xi, \boldsymbol{\pi}; t)$. In the Zwanzig-like formal projection approach,[30,50,67] we use the identity $\rho(h, T, \xi, \boldsymbol{\pi}; t) = (\mathbb{Q} + \mathbb{P})\rho(h, T, \xi, \boldsymbol{\pi}; t)$, where $\mathbb{Q} = 1 - \mathbb{P}$; we apply separately $\mathbb{P}$ and $\mathbb{Q}$ to Eq. (A2) and obtain a couple of differential equations. Then, from this couple of differential equations, we obtain the equation of motion for the $\sigma(h, T; t)$. This hides the dynamics of the booster part. Considering that we are observing the system of interest for times much longer than the decay times of the correlation functions of the booster, we get rid of the initial PDF. Consequently, the evolution of the PDF of the system of interest $\sigma(h, T; t)$ is no longer deterministic. At the lowest nonvanishing order of the coupling parameter ϵ, the time evolution of $\sigma(h, T; t)$ obeys the following integro-differential equation

$$\begin{aligned} \partial_t \sigma(\boldsymbol{x}; t) &= \mathcal{L}_a\, \sigma(\boldsymbol{x}; t) \\ &\quad + \epsilon^2\, \langle \xi^2 \rangle_b \left\{ \mathcal{L}_I \int_0^\infty \mathrm{d}u\, \varphi(u)\, e^{\mathcal{L}_a u} \mathcal{L}_I e^{-\mathcal{L}_a u} \right\} \sigma(\boldsymbol{x}; t), \end{aligned} \tag{A4}$$

where $\varphi(u)$ is the normalized auto-correlation function of the booster variable ξ and $\langle \xi^2 \rangle_b$ is the variance of ξ (without loss of generality, we assume $\langle \xi \rangle_b = 0$).

Equation (A4) implies that *we can group all the possible booster dynamical systems in different classes of equivalence, where all the booster belonging to the same class give rise to the same statistical properties for a given system of interest*. In fact, the FPE depends only on the booster autocorrelation function $\langle \xi^2 \rangle_b \varphi(u)$: different dynamical systems that share the same autocorrelation function belong to the same booster class of equivalence. Given Eq. (A3), we can rewrite Eq. (A4) as

$$\begin{aligned} \partial_t \sigma(h, T; t) = \Big\{ & \partial_h \omega\, T - \partial_T \omega\, h + \lambda\, \partial_T T \\ & + \beta\, \epsilon^2\, \langle \xi^2 \rangle_b\, \tau\, \partial_T (1 + \beta\, T) \\ & + \epsilon^2\, \langle \xi^2 \rangle_b\, \partial_T (1 + \beta\, T) \\ & \times \int_0^\infty \mathrm{d}u\, \varphi(u)[1 + \beta\, T_a(h, t; -u)] \\ & \times e^{\mathcal{L}_a u} \partial_T e^{-\mathcal{L}_a u} \Big\}\, \sigma(h, T; t), \end{aligned} \tag{A5}$$

where we have used the identity $\partial_T(1 + \beta\, T) = (1 + \beta\, T)\partial_T + \beta$ (the interaction with the booster is not Hamiltonian) and we have introduced the decay time of the booster

autocorrelation function defined as $\tau \equiv \int_0^\infty du\varphi(u)$. In Eq. (A5), we have exploited the result $\exp[\mathcal{L}_a u]T\exp[-\mathcal{L}_a u] = T_a(h,t;-u)$ [see, for example, Eqs. (31) and (32) of Ref. 21], where $T_a(h,t;-u)$ and $h_a(h,t;-u)$ are the unperturbed ($\epsilon = 0$) back time evolution for a time u of the T and the h variables, respectively, starting from the initial condition $T_a(h,t;0) = T$ and $h_a(h,t;0) = h$, up to the time $-u$.

Notice that the last drift term of Eq. (A5), proportional to β, is due to the fact that the interaction of the booster variable ξ with the ROM is not Hamiltonian, in fact it depends on the variable T that plays the role of the velocity if we consider the ROM as a standard harmonic oscillator. Incidentally, this term is formally equivalent to the "noise-induced drift" involved in the Itô vs Stratonovich debate about the interpretation of SDE.

2. The general FPE for the ROM

From Eq. (A5), we can obtain the transport coefficients $A(h,T)$ and $B(h,T)$ of Eq. (3) for the general case, when we do not make any assumptions about the time scale separation between the ROM and the booster. Although we already reported them in B_15, to make this paper self consistent, we shall obtain again the expressions for $A(h,T)$ and $B(h,T)$.

The most troublesome term is $\exp[\mathcal{L}_a u]\partial_T \exp[-\mathcal{L}_a u]$ inside the integral of Eq. (A5). In general, this expression gives rise to a series of differential operators, which needs to be summed. For Hamiltonian systems of interest the unperturbed Loiuville operator $\mathcal{L}_a$ preserves the energy and can be written in terms of Poisson brackets. In this case, the series was resummed some years ago,[30] and the coefficients of the corresponding diffusion operator were obtained. More recently, in B_15 the series was resummed also in the case of dissipative systems of interest, resulting the following first order partial differential operator

$$\begin{aligned} e^{\mathcal{L}_a u}\partial_T e^{-\mathcal{L}_a u} &= e^{-\lambda u}[\partial_T h_a(h,t;-u)]\partial_h \\ &\quad + e^{-\lambda u}[\partial_h h_a(h,t;-u)]\partial_T. \end{aligned} \tag{A6}$$

In the case of the LOM in Eq. (A1), the system of interest is the ROM and its unperturbed evolution is easily obtained as

$$\begin{aligned} h_a(h,t;-u) &= e^{\frac{\lambda}{2}u}\left[\cos(\Omega u) - \frac{\lambda}{2}\frac{\sin(\Omega u)}{\Omega}\right]h \\ &\quad + e^{\frac{\lambda}{2}u}\,\omega\frac{\sin(\Omega u)}{\Omega}\,T \\ T_a(h,t;-u) &= -e^{\frac{\lambda}{2}u}\,\omega\frac{\sin(\Omega u)}{\Omega}\,h \\ &\quad + e^{\frac{\lambda}{2}u}\left[\cos(\Omega u) + \frac{\lambda}{2}\frac{\sin(\Omega u)}{\Omega}\right]T, \end{aligned} \tag{A7}$$

where $\Omega \equiv \sqrt{\omega^2 - (\frac{\lambda}{2})^2}$, leading to

$$\begin{aligned} (\partial_h h_a[h,t;-u]) &= e^{\frac{\lambda}{2}u}\left[\cos(\Omega u) - \frac{\lambda}{2}\frac{\sin(\Omega u)}{\Omega}\right] \\ (\partial_T h_a[h,t;-u]) &= e^{\frac{\lambda}{2}u}\,\omega\frac{\sin(\Omega u)}{\Omega}. \end{aligned} \tag{A8}$$

Thus, using Eqs. (A6)–(A8), we see that the last line in the r.h.s. of Eq. (A5) is a second order differential operator, with coefficients that are quadratic polynomials of the ROM variables (h,T). Namely, Eq. (A5) becomes the FPE given in Eqs. (3) and (4), where (we remind that $D \equiv \epsilon^2\langle\xi^2\rangle_b\tau$)

$$\begin{aligned} A_0 &= \frac{D}{\tau}\int_0^\infty du\,\varphi(u)e^{-\frac{\lambda}{2}u}\left[\cos(\Omega u) - \frac{\lambda}{2\Omega}\sin(\Omega u)\right] \\ &= \frac{D}{\tau}\left\{\Re\left[\hat\varphi(\Omega - i\lambda/2)\right] + \frac{\lambda}{2\Omega}\Im\left[\hat\varphi(\Omega - i\lambda/2)\right]\right\}, \end{aligned} \tag{A9}$$

$$\begin{aligned} A_1 &= -\frac{D}{\tau}\,\frac{\omega}{2\Omega}\int_0^\infty du\,\varphi(u)\left[\frac{\lambda}{2\Omega}\cos(2\Omega u) + \sin(2\Omega u)\right] \\ &\quad + \frac{D}{\tau}\,\frac{\omega\lambda}{4\Omega^2}\int_0^\infty \varphi(u)du \\ &= -\frac{D}{\tau}\,\frac{\omega}{2\Omega}\left\{\frac{\lambda}{2\Omega}\Re\left[\hat\varphi(2\Omega)\right] - \Im\left[\hat\varphi(2\Omega)\right]\right\} + D\,\frac{\omega\lambda}{4\Omega^2}, \end{aligned} \tag{A10}$$

$$\begin{aligned} A_4 &= \frac{D}{\tau}\int_0^\infty du\,\varphi(u)\left[\omega^2(1+\cos(2\Omega u)) - \frac{\lambda^2}{2}\right]\frac{1}{2\Omega^2} \\ &= D\left(1 - \frac{\omega^2}{2\Omega^2}\right) + \frac{D}{\tau}\,\frac{\omega^2}{2\Omega^2}\Re\left[\hat\varphi(2\Omega)\right], \end{aligned} \tag{A11}$$

$$A_2 = A_4 + A_0, \quad A_3 = A_1, \tag{A12}$$

$$\begin{aligned} B_0 &= -\frac{D}{\tau}\,\frac{\omega}{\Omega}\int_0^\infty du\,\varphi(u)e^{-\frac{\lambda}{2}u}\sin(\Omega u) \\ &= \frac{D}{\tau}\,\frac{\omega}{\Omega}\Im\left[\hat\varphi(\Omega - i\lambda/2)\right], \end{aligned} \tag{A13}$$

$$\begin{aligned} B_1 &= -\frac{D}{\tau}\,\frac{\omega^2}{2\Omega^2}\int_0^\infty du\,\varphi(u)\cos(2\Omega u) \\ &\quad + \frac{D}{\tau}\,\frac{\omega^2}{2\Omega^2}\int_0^\infty \varphi(u)du \\ &= -\frac{D}{\tau}\,\frac{\omega^2}{2\Omega^2}\Re\left[\hat\varphi(2\Omega)\right] + D\,\frac{\omega^2}{2\Omega^2}, \end{aligned} \tag{A14}$$

$$\begin{aligned} B_4 &= -\frac{D}{\tau}\,\frac{\omega}{2\Omega}\int_0^\infty du\,\varphi(u)\left[\sin(2\Omega u) - \frac{\lambda}{\Omega}\cos(2\Omega u)\right] \\ &\quad - \frac{D}{\tau}\,\frac{\lambda}{2}\,\frac{\omega}{\Omega^2}\int_0^\infty \varphi(u)du \\ &= \frac{D}{\tau}\,\frac{\omega}{2\Omega}\left\{\frac{\lambda}{\Omega}\Re\left[\hat\varphi(2\Omega)\right] + \Im\left[\hat\varphi(2\Omega)\right]\right\} \\ &\quad - D\,\frac{\lambda}{2}\,\frac{\omega}{\Omega^2}, \end{aligned} \tag{A15}$$

$$B_2 = B_4 + B_0, \quad B_3 = B_1, \tag{A16}$$

with $\tau = \Re\left[\hat\varphi(0)\right]$; the symbols $\Im[\ldots]$ and $\Re[\ldots]$ stand for the imaginary and the real part of $[\ldots]$, respectively, and the hat over the function φ means the Fourier transform of this function, having assumed $\varphi(t) = 0$ for $t < 0$:

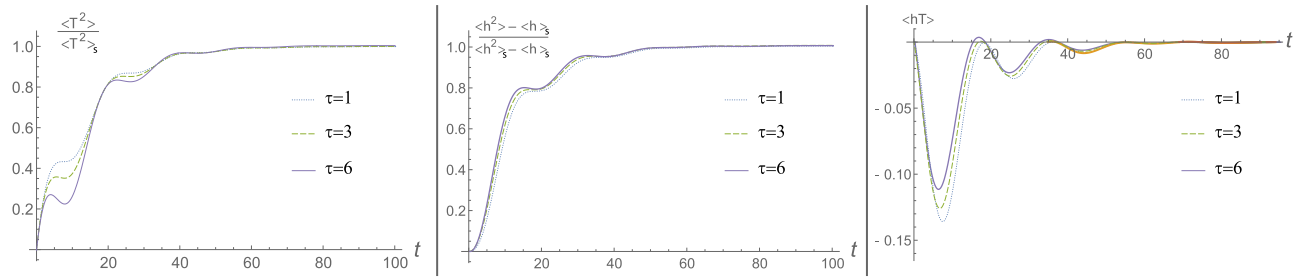

FIG. 10. Evolution of the variance of T (left), h (center) and of the cross-correlation between T and h, obtained from Eq. (A19) with the A_i and B_i coefficients given by Eqs. (A9)–(A16), in the case where $\varphi(t) = \exp(-t/\tau)$, for different values of τ. Solid line: $\tau = 6$; dashed line: $\tau = 3$; dotted line: $\tau = 1$. Curves for different values of τ are very similar.

$\hat{\varphi}(k) \equiv \int_0^\infty \exp[-iku]\varphi(u)\mathrm{d}u$. Notice also that the following equalities hold

$$A_4 + B_3 = D, \quad A_2 + B_1 = A_0 + D. \tag{A17}$$

In the limit of large time scale separation between the ROM and the booster, we can use the approximations $\Re\left[\hat{\varphi}(x\,\Omega)\right] \sim \Re\left[\hat{\varphi}(0)\right] = \tau$ and $\Im\left[\hat{\varphi}(x\,\Omega)\right] \sim \Im\left[\hat{\varphi}(0)\right] = 0$ in Eqs. (A9)–(A16).

3. The dynamics of the first two moments

Using the FPE of Eqs. (3) and (4), it is easy to obtain a closed equation of motion of the first n-th moments of the ROM. For the first two moments we get

$$\begin{aligned}
\langle \dot{h} \rangle &= -\omega \langle T \rangle, \\
\langle \dot{T} \rangle &= (\omega + \beta^2 A_3) \langle h \rangle - (\lambda - \beta^2 A_4) \langle T \rangle + \beta A_0,
\end{aligned} \tag{A18}$$

$$\begin{aligned}
\langle \dot{h^2} \rangle &= -2\omega \langle hT \rangle, \\
\langle h\dot{T} \rangle &= (\omega + \beta^2 A_3) \langle h^2 \rangle \\
&\quad - (\lambda - \beta^2 D) \langle hT \rangle - (\omega - \beta^2 B_4) \langle T^2 \rangle \\
&\quad + \beta (D + A_0 - A_4) \langle h \rangle - \beta B_2 \langle T \rangle + B_0, \\
\langle \dot{T^2} \rangle &= 2(\omega + 2\beta^2 A_3) \langle hT \rangle - 2 \left(\lambda - \beta^2 2A_4\right) \langle T^2 \rangle \\
&\quad + 2\beta (2A_0 + A_4) \langle T \rangle + 2\beta A_3 \langle h \rangle + 2A_0.
\end{aligned} \tag{A19}$$

From which

$$\begin{aligned}
\langle T^2 \rangle_{eq} &= \frac{A_0}{\lambda - 2\beta^2 A_4} \left(1 - \frac{\beta^2 A_3}{\beta^2 A_3 + \omega}\right) \\
&\approx \frac{A_0}{\lambda} \left[1 + \beta^2 \left(2\frac{A_0}{\lambda} - \frac{A_3}{\omega}\right)\right] + O(\epsilon^6) \approx \frac{A_0}{\lambda} + O(\epsilon^4).
\end{aligned} \tag{A20}$$

Thus, the width of the stationary PDF is well approximated by the width of the Gaussian PDF we had if $\beta = 0$.

A few comments are appropriate: Eq. (A18) depends only on the A transport coefficient of the FPE and it is equivalent to the equation of motion of a linear dissipative oscillator, with bare frequency $\sqrt{\omega(\omega + \beta^2 A_3)}$ and friction coefficient $(\lambda - \beta^2 A_4)$, perturbed by the constant force βA_0. The weak perturbation assumption and the fact that $\beta \sim 0.2$, imply that $\omega + \beta^2 A_3 \sim \omega$ and $(\lambda - \beta^2 A_4) \sim \lambda$.

Concerning the second moments equation of motion of Eq. (A19), similarly, they weakly depend on B and they mainly depend on β, and A_0, thus, the dynamics of the second moments should not depend too much on the time scale of the booster [see Fig. 10].

Assuming an exponential decays of the autocorrelation function of ξ, i.e., $\varphi(t) = \exp(-t/\tau)$, we have that for values of τ up to $\sim 3\,\text{months}^{-1}$, the transport coefficient A has the same structure it has in the limit of very large time scale separation between the dynamics of the unperturbed ROM and that of the perturbation $\xi(t)$: $A_1 = A_3 \sim 0$, $A_0 \sim A_2/2 \sim A_4$, namely, $A(T) \sim A_0\,(1 + \beta T)^2$ (see Fig. 11).

Because $\lambda = 1/12\,\text{months}^{-1}$, for $\tau = 3\,\text{months}^{-1}$, we have a large, but *not very* large time scale separation between the dynamics of the unperturbed ROM and that of the perturbation $\xi(t)$.

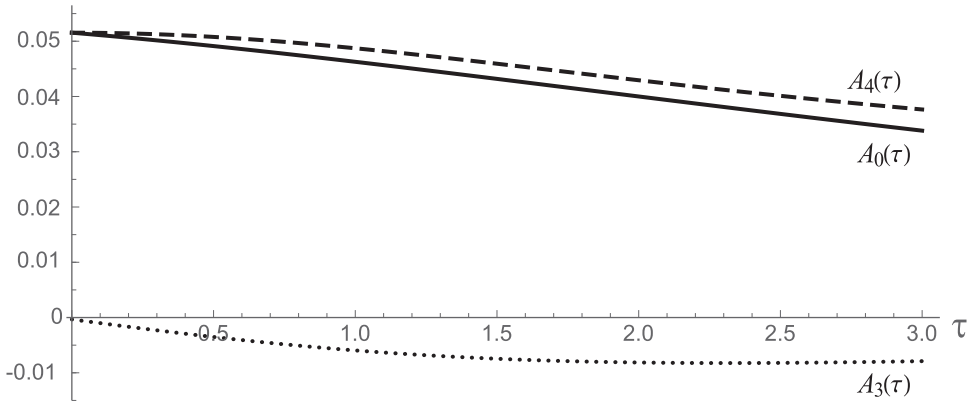

FIG. 11. The values of the coefficients A_0, A_4, and A_3 vs τ for $\varphi(t) = \exp(-t/\tau)$. In the range $0 \le \tau \le 3$, we have $A_4 \sim A_0$ and $A_3 \sim 0$. We recall that $A_2 = A_4 + A_0$ and that $A_1 = A_3$. Thus $A \sim A_0(1 + \beta T)^2$, which must be compared with $A = D(1 + \beta T)^2$ that holds true in the limit of very large time scale separation between the dynamics of the ROM and that of the booster (see text for details).

4. The case of large time scale separation

We can now extend the work in B_16: using Eq. (A1) as a LOM mimicking the statistics of the ENSO, we can safely stay in the limit of very large time scale separation between the dynamics of the ROM and that of the booster. The coefficients of the FPE in this limit case are given by Eqs. (A9)–(A17) considering the limit of vanishing frequency in the Fourier transform of φ ($\Re\left[\hat{\varphi}(0)\right] = \tau$ and $\Im\left[\hat{\varphi}(0)\right] = 0$), from which $A_1 \sim A_3 \sim 0\,, A_0 \sim A_2/2 \sim A_4 \sim D \equiv \epsilon^2 \langle \xi^2 \rangle_b \tau$. Alternatively, the FPE can be directly obtained from Eq. (A5), considering that in this case in the integral of the last line the booster autocorrelation function $\varphi(u)$ decays so fast, with respect to the typical time scale of the unperturbed ROM, that we can make the approximations $T_a(h,t;-u) \sim T$ and $e^{\mathcal{L}_a u}\partial_T e^{-\mathcal{L}_a u} \sim \partial_T$. In both approaches, we eventually obtain

$$\begin{aligned}\partial_t \sigma(h,T;t) = \big\{&\omega\,\partial_h T - \omega\,\partial_T h + \lambda\,\partial_T T \\ &+ D\,\beta\,\partial_T(1+\beta\,T) \\ &+ D\,\partial_T(1+\beta\,T)^2\partial_T\big\}\sigma(h,T;t),\end{aligned} \tag{A21}$$

which, after elementary algebraic manipulation, coincides with the FPE of Eq. (7).

APPENDIX B: THE ANSATZ AND THE STATIONARY PDF

Here, we review Appendix B of B_16, to find the reduced stationary PDF for the T variable. We start from the corrected FPE of Eq. (A21) or the equivalent of Eq. (7). First of all, note that the second line in Eq. (A21) corresponds to the a term (is missing in B_16). This term (weakly) changes the effective friction of the perturbed ROM from λ to $\lambda + D\beta^2$, and it introduces also an effective constant forcing, $-D\beta$, on the perturbed ROM. It is straightforward to check that this constant force halves the stationary value of the average of the h variable, respect to that obtained in B_16. We have

$$\langle h \rangle_s = -D\frac{\beta}{\omega}, \tag{B1}$$

a result that we shall use hereafter. Because we are interested only on the reduced PDF for the T variable, we integrate the h variable in the FPE of Eq. (A21), to obtain

$$\begin{aligned}\partial_t p(T;t) = -\omega\,\partial_T\langle h\rangle_T + \big\{&D\beta\partial_T + (\lambda + D\beta^2)\partial_T T \\ &+\partial_T D(1+\beta T)^2\partial_T\big\}\,p(T;t),\end{aligned} \tag{B2}$$

where $p(T;t) \equiv \int \sigma(h,T;t)\mathrm{d}h$ is the reduced PDF for the T variable and $\langle h\rangle_T \equiv \int h\sigma(h,T;t)\mathrm{d}h$, is the conditional average value of the h variable [note: $p_s(T) \equiv \int \sigma_s(h,T)\mathrm{d}h$]. Because $\omega \sim 0.13$ and $\lambda \sim 0.1$, we are neither in the under-damped nor in the over-damped standard cases, where it is possible to reduce the two-dimensional FPE to the one dimensional type.[49,50,68] However, we take advantage of the fact that here we focus our attention on the *stationary* PDF of the reduced FPE, for which $\partial p(T;t)/\partial t = 0$ in Eq. (B2). Thus, observing that the relations among the stationary first and second moments of the h and T variables that we obtain from the FPE of Eq. (A21), are the same of the case of a stochastic forced damped linear oscillator (see also B_16), we make the following *ansatz*

$$\langle h\rangle_{T,s} = \langle h\rangle_s\, p_s(T) = -\beta\frac{D}{\omega}\,p_s(T), \tag{B3}$$

where the former equality represents the ansatz, and in the latter we exploited Eq. (B1).

Inserting Eq. (B3) in the FPE of Eq. (B2), imposing the condition of vanishing current, and using the definition $\mu \equiv 1 + \lambda/(D\,\beta^2)$, we obtain

$$\beta(2+\mu\,\beta T)\,p_s(T) + (1+\beta T)^2\partial_T\,p_s(T) = 0. \tag{B4}$$

From the previous equation, we get two results: the stationary PDF has a maximum (i.e., the T derivative vanishes) for $T = -2/(\beta\mu) = -2\beta D/(\lambda + D\,\beta^2)$; the stationary PDF must vanish for $T = -1/\beta$ (and for lesser values too, for obvious physical reasons). As already noted in B_16, from the FPE of Eq. (A21), we see that for $\mu > 3$ the equation of motion of the first and second order moments of the ROM converge to a finite value for $t \to \infty$. It is not difficult to check that the same constraint ensures that also the solution of the same FPE converges, for $t \to \infty$, to a finite (normalizable) stationary PDF. Thus, under the assumption that $\mu > 3$, from Eq. (B4) we get the stationary PDF given in Eq. (8).

APPENDIX C: ANALYTIC EXPRESSION FOR THE MEAN FPT

1. The ansatz at work for the calculation of the FPT

In the state space of (h,T), we assume an absorbing boundary $T = T_{tg}$ for the paths starting from the initial region $-0.5 \le h_i \le 0.5$, $-0.5 \le T_i \le 0.5$, and we indicate with $\wp(h_i,T_i \mid T_{tg};\delta t)$ the PDF of the FPT of these paths. Given the FPE in Eq. (7), it is easy to prove that $\wp(h_i,T_i \mid T_{tg};\delta t)$ satisfies the adjoint FPE[57,58]

$$\begin{aligned}\partial_{\delta t}\,\wp(h_i,T_i \mid T_{tg};\delta t) = \{&-\omega T_i\partial_{h_i} + \omega h_i\partial_{T_i} - (\lambda + D\beta^2)T_i\partial_{T_i} \\ &- D\beta\partial_T + \partial_{T_i}A(T)\partial_{T_i}\}\wp(h_i,T_i \mid T_{tg};\delta t),\end{aligned} \tag{C1}$$

where we want to remove the h_i dependence. For this purpose, we define $\mathcal{P}_{st}(h)$ as the reduced stationary PDF for the variable h, we multiply Eq. (C1) by $\mathcal{P}_{st}(h_i)$ and we integrate over h_i

$$\begin{aligned}&\partial_{\delta t}\int \wp(h_i,T_i \mid T_{tg};\delta t)\mathcal{P}_{st}(h_i)\mathrm{d}h_i = \\ &-\omega T_i\left(\int \mathcal{P}_{st}(h_i)\partial_{h_i}\,\wp(h_i,T_i \mid T_{tg};\delta t)\mathrm{d}h_i\right) \\ &+\partial_{T_i}\,\omega\left(\int \mathcal{P}_{st}(h_i)h_i\,\wp(h_i,T_i \mid T_{tg};\delta t)\mathrm{d}h_i\right) \\ &-(\lambda + D\beta^2)T_i\partial_{T_i}\,\wp(T_i \mid T_{tg};\delta t) - D\beta\partial_{T_i}\,\wp(T_i \mid T_{tg};\delta t) \\ &+\partial_{T_i}A(T_i)\partial_{T_i}\wp(T_i \mid T_{tg};\delta t),\end{aligned} \tag{C2}$$

where $\wp(T_i \mid T_{tg};\delta t) \equiv \int \wp(h_i,T_i \mid T_{tg};\delta t)dh_i$. Now, we know that if the starting position (h_i,T_i) belongs to a neighborhood of points (h,T), where the PDF is close to the maximum value, the FPT should not depend too much on (h_i,T_i). Assuming that this is the case, the l.h.s. of the previous equation becomes $\partial_{\delta t}\,\wp(T_i \mid T_{tg};\delta t)$, while in the r.h.s. the first term vanishes, and inside the integral of the second one we

can make the substitution $\wp(h_i, T_i \mid T_{tg}; \delta t) \sim \wp(T_i \mid T_{tg}; \delta t)$ [because $\mathcal{P}_{st}(h_i)$ is peaked closed to $h_i = 0$]. Thus we get

$$\begin{aligned}\partial_{\delta t}\,\wp(T_i \mid T_{tg}; \delta t) &= \omega\langle h\rangle_s \partial_{T_i}\wp(T_i \mid T_{tg}; \delta t)\\ &- (\lambda + D\beta^2) T_i \partial_{T_i}\wp(T_i \mid T_{tg}; \delta t)\\ &- D\beta\partial_{T_i}, \wp(T_i \mid T_{tg}; \delta t) + \partial_{T_i} A(T_i)\partial_{T_i}\wp(T_i \mid T_{tg}; \delta t),\end{aligned} \tag{C3}$$

where $\langle h\rangle_s$ is the stationary value of h. Using Eq. (B1), formally the above equation is equal to the adjoint of the following FPE for the reduced PDF of the sole T variable

$$\begin{aligned}&\partial_t p(T;t)\\ &= \left\{(\lambda + D\beta^2)\partial_T T + 2D\beta\partial_{T_i} + \partial_T A(T_i)\partial_T\right\} p(T;t).\end{aligned} \tag{C4}$$

Imposing the stationary condition in the Eq. (C4) we get Eq. (B4). Thus Eq. (C3) can be thought as derived from a one-dimensional stochastic process governed by the FPE of Eq. (C4), for which the stationary solution is given in Eq. (8). It is well known[57,58] that from such a one-dimensional FPE we get directly the expressions in Eqs. (11) and (12) for the mean FPT and for the second moment of the FPT.

2. Analytic expression for the mean FPT

Substituting the stationary PDF of Eq. (8), in the expression for the average FPT given in Eq. (11), we have

$$t_1(T_i \mid T_{tg}) = \int_{T_i}^{T_{tg}} \frac{\mathrm{d}T}{D(1+\beta T)^2 p_s(T)} \frac{\Gamma\left(\mu - 1, \frac{\mu-2}{\beta T+1}\right)}{\Gamma(\mu-1)}, \tag{C5}$$

where $\Gamma(a,x)$ is the standard incomplete Gamma function. For $T_{tg} > 1$, with a good approximation, the factor $\Gamma\left(\mu - 1, \frac{\mu-2}{\beta T+1}\right)/\Gamma(\mu-1)$ in the integrand of Eq. (C5), can be substituted by one (see Fig. 12).

This approximation leads to a relative error that ranges from less than 3% for $T_{tg} \geq 2.5$ to 15% for $T_{tg} = 1$. Using this approximation and making the change of variable

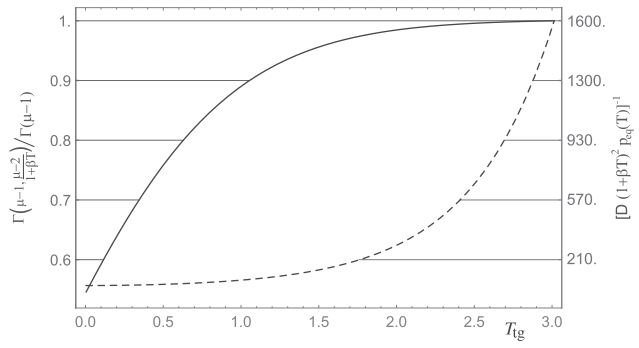

FIG. 12. Plot of the two factors, $\Gamma\left(\mu - 1, \frac{\mu-2}{\beta T+1}\right)/\Gamma(\mu-1)$ (solid line, with values on the left vertical axis) and $1/[D(1+\beta T)^2 p_s(T)]$ (dashed line, with values on the right vertical axis), which appear into the integral of Eq. (C5). It is clear from these graphs that for $T > 1$ the first factor $\Gamma\left(\mu - 1, \frac{\mu-2}{\beta T+1}\right)/\Gamma(\mu-1)$ can be approximated by the unity, while for $T < 1$ the product of these two factors is relatively small, thus it gives a far lesser contribute to the integral. We can conclude that for $T_{tg} > 1$ in Eq. (C5) we can safely make the following substitution: $\Gamma\left(\mu - 1, \frac{\mu-2}{\beta T+1}\right)/\Gamma(\mu-1) \to 1$.

$x = (\mu-2)(\beta T+1)$, we have

$$\begin{aligned}t_1(T_i \mid T_{tg}) &= \frac{\Gamma(\mu-1)}{\beta^2 D}\int_{\frac{\mu-2}{\beta T_{tg}+1}}^{\frac{\mu-2}{\beta T_i+1}} e^x x^{-\mu}\mathrm{d}x\\ &= \frac{\Gamma(\mu-1)}{\beta^2 D}(-1)^\mu \left\{\Gamma(1-\mu,-x)\right\}_{\frac{\mu-2}{\beta T_i+1}}^{\frac{\mu-2}{\beta T_{tg}+1}}.\end{aligned} \tag{C6}$$

This expression is not easily handled because of the complex number $(-1)^\mu$ and because the incomplete Gamma function has a non-analytical behavior when its arguments assume negative values, thus we exploit the following identity: $\Gamma(a,z) = \exp[-z]\Psi(1-a, 1-a; z)$, where $\Psi(b,c;z)$ is the Tricomi confluent hypergeometric function. In turn, the Tricomi function can be expressed in term of the Kummer generalized hypergeometric function: $\Psi(b,c;z) = M(b,c;z)\Gamma(1-c)/\Gamma(b-c+1) + z^{1-c}M(b-c+1, 2-c; z)\Gamma(c-1)/\Gamma(c)$. Using these identities, we rewrite Eq. (C6) in the following way

$$\begin{aligned}t_1(T_i \mid T_{tg}) = \frac{\Gamma(\mu-1)}{\beta^2 D}\Big\{&(-1)^{\mu-1}\Gamma(1-\mu)\, e^x M(\mu,\mu,-x)\\ &+ \frac{x^{1-\mu}}{\mu-1} e^x M(1, 2-\mu, -x)\Big\}_{\frac{\mu-2}{\beta T_i+1}}^{\frac{\mu-2}{\beta T_{tg}+1}}.\end{aligned} \tag{C7}$$

Because $M(\mu,\mu,-x) = \exp(-x)$, the first term inside the big brackets of Eq. (C7) is a constant and can be neglected being at least two order of magnitude lesser than the second one for the range $\frac{\mu-2}{\beta T_{tg}+1} \leq x \leq \frac{\mu-2}{\beta T_i+1}$. Thus, using also the expression in Eqs. (8)–(10) for the stationary PDF, and the identity $1/D = (\mu-1)\beta^2/\lambda$, we get the good approximation for the mean FPT given in Eq. (13). As it can be checked by numerical integration, the deviation of this approximation from the exact mean FPT in Eq. (11) ranges from a maximum of 17% for $T_{tg} = 1$ to less then 1% for $T_{tg} > 3.5$.

[1] S. Curtis, R. F. Adler, G. J. Huffman, G. Gu, D. T. Bolvin, and E. J. Nelkin, "Comments on 'El Ni no: Catastrophe or opportunity'," J. Clim. **19**, 6439–6442 (2006).
[2] A. Capotondi, A. T. Wittenberg, M. Newman, E. D. Lorenzo, J.-Y. Yu, P. Braconnot, J. Cole, B. Dewitte, B. Giese, E. Guilyardi, F.-F. Jin, K. Karnauskas, B. Kirtman, T. Lee, N. Schneider, Y. Xue, and S.-W. Yeh, "Understanding enso diversity," Bull. Am. Meteorol. Soc. **96**, 921–938 (2015).
[3] A. Capotondi, "El Nin o southern oscillation ocean dynamics: Simulation by coupled general circulation models," in *Climate Dynamics: Why Does Climate Vary?* (American Geophysical Union, 2013), pp. 105–122.
[4] F.-F. Jin, "An equatorial ocean recharge paradigm for ENSO. Part II: A stripped-down coupled model," J. Atmos. Sci. **54**, 830–847 (1997a).
[5] F.-F. Jin, "An equatorial ocean recharge paradigm for ENSO. Part I: Conceptual model," J. Atmos. Sci. **54**, 811–829 (1997b).
[6] C. S. Meinen and M. J. McPhaden, "Observations of warm water volume changes in the equatorial pacific and their relationship to el nio and la nia," J. Clim. **13**, 3551–3559 (2000).
[7] A. Capotondi, A. Wittenberg, and S. Masina, "Spatial and temporal structure of tropical pacific interannual variability in 20th century coupled simulations," Ocean Model. **15**, 274–298 (2006).
[8] H.-L. Ren and F.-F. Jin, "Recharge oscillator mechanisms in two types of enso," J. Clim. **26**, 6506–6523 (2013).
[9] A. Capotondi, "Enso diversity in the ncar ccsm4 climate model," J. Geophys. Res. Oceans **118**, 4755–4770 (2013b).
[10] M. J. McPhaden, "Genesis and evolution of the 1997-98 el niño," Science **283**, 950–954 (1999).
[11] A. V. Fedorov, "The response of the coupled tropical ocean atmosphere to westerly wind bursts," Q. J. R. Meteorol. Soc. **128**, 1–23 (2002).
[12] M. Puy, J. Vialard, M. Lengaigne, and E. Guilyardi, "Modulation of equatorial pacific westerly/easterly wind events by the Madden–Julian oscillation

and convectively-coupled Rossby waves," Clim. Dyn. **46**, 2155–2178 (2016).
[13]L. Yu, R. A. Weller, and W. T. Liu, "Case analysis of a role of ENSO in regulating the generation of westerly wind bursts in the western equatorial pacific," J. Geophys. Res. Oceans **108**, 3128 (2003).
[14]I. Eisenman, L. Yu, and E. Tziperman, "Westerly wind bursts: ENSOs tail rather than the dog?" J. Clim. **18**, 5224–5238 (2005).
[15]G. Gebbie, I. Eisenman, A. Wittenberg, and E. Tziperman, "Modulation of westerly wind bursts by sea surface temperature: A semistochastic feedback for enso," J. Atmos. Sci. **64**, 3281–3295 (2007).
[16]P. Sura, "On non-gaussian sst variability in the gulf stream and other strong currents," Ocean Dyn. **60**, 155–170 (2010).
[17]P. Sura, "A general perspective of extreme events in weather and climate," Atmos. Res. **101**, 1–21 (2011).
[18]F.-F. Jin, L. Lin, A. Timmermann, and J. Zhao, "Ensemble-mean dynamics of the ENSO recharge oscillator under state-dependent stochastic forcing," Geophys. Res. Lett. **34**, L03807 (2007).
[19]A. F. Z. Levine and F.-F. Jin, "Noise-induced instability in the ENSO recharge oscillator," J. Atmos. Sci. **67**, 529–542 (2010).
[20]M. Bianucci, "Nonconventional fluctuation dissipation process in non-Hamiltonian dynamical systems," Int. J. Modern Phys. B **30**, 1541004 (2015a).
[21]M. Bianucci, "On the correspondence between a large class of dynamical systems and stochastic processes described by the generalized Fokker Planck equation with state-dependent diffusion and drift coefficients," J. Stat. Mech. Theor. Exp. **2015**, P05016 (2015b).
[22]M. Bianucci, "Large scale emerging properties from non Hamiltonian complex systems," Entropy **19** (2017).
[23]M. Bianucci and S. Merlino, *Non Standard Fluctuation Dissipation Processes in Ocean-Atmosphere Interaction and for General Hamiltonian or Non Hamiltonian Phenomena: Analytical Results* (Nova Science Publisher, 2017).
[24]M. Bianucci, "Analytical probability density function for the statistics of the ENSO phenomenon: Asymmetry and power law tail," Geophys. Res. Lett. **43**, 386–394 (2016).
[25]A. Moore and R. Kleeman, "The dynamics of error growth and predictability in a coupled model of ENSO," Q. J. R. Meteorol. Soc. **122**, 1405–1446 (1996).
[26]C. Penland and P. D. Sardeshmukh, "The optimal growth of tropical sea surface temperature anomalies," J. Clim. **8**, 1999–2024 (1996).
[27]J. B. Weiss, "Fluctuation properties of steady-state Langevin systems," Phys. Rev. E **76**, 061128 (2007).
[28]G. Burgers, F.-F. Jin, and G. J. van Oldenborgh, "The simplest ENSO recharge oscillator," Geophys. Res. Lett. **32**, L13706 (2005).
[29]M. Bianucci, R. Mannella, X. Fan, P. Grigolini, and B. J. West, "Standard fluctuation-dissipation process from a deterministic mapping," Phys. Rev. E **47**, 1510–1519 (1993).
[30]M. Bianucci, R. Mannella, B. J. West, and P. Grigolini, "From dynamics to thermodynamics: Linear response and statistical mechanics," Phys. Rev. E **51**, 3002–3022 (1995).
[31]C. Zhang and J. Gottschalck, "SST anomalies of ENSO and the Madden-Julian oscillation in the equatorial pacific," J. Clim. **15**, 2429–2445 (2002).
[32]R. C. Y. Li, W. Zhou, J. C. L. Chan, and P. Huang, "Asymmetric modulation of Western North Pacific cyclogenesis by the Madden-Julian oscillation under ENSO conditions," J. Clim. **25**, 5374–5385 (2012).
[33]J. Zavala-Garay, C. Zhang, A. M. Moore, and R. Kleeman, "The linear response of ENSO to the Madden-Julian oscillation," J. Clim. **18**, 2441–2459 (2005).
[34]H. H. Hendon, M. C. Wheeler, and C. Zhang, "Seasonal dependence of the MJO-ENSO relationship," J. Clim. **20**, 531–543 (2007).
[35]H. A. Dijkstra and G. Burgers, "Fluid dynamics of el Ni no variability," Annu. Rev. Fluid. Mech. **34**, 531–558 (2002).
[36]P. D. Sardeshmukh and C. Penland, "Understanding the distinctively skewed and heavy tailed character of atmospheric and oceanic probability distributions," Chaos **25**, 036410 (2015).
[37]P. D. Sardeshmukh and P. Sura, "Reconciling non-gaussian climate statistics with linear dynamics," J. Clim. **22**, 1193–1207 (2009).
[38]P. Sura and P. D. Sardeshmukh, "A global view of air-sea thermal coupling and related non-gaussian {SST} variability," Atmos. Res. **94**, 140–149 (2009).
[39]P. D. Sardeshmukh, G. P. Compo, and C. Penland, "Need for caution in interpreting extreme weather statistics," J. Clim. **28**, 9166–9187 (2015).
[40]C. Penland and P. D. Sardeshmukh, "Alternative interpretations of power-law distributions found in nature," Chaos **22**, 023119 (2012).
[41]R. Khasminskii, "A limit theorem for the solutions of differential equations with random right-hand sides," Theor. Prob. Appl. **11**, 390–406 (1966).
[42]G. Gallavotti and E. G. D. Cohen, "Dynamical ensembles in stationary states," J. Stat. Phys. **80**, 931–970 (1995a).
[43]G. Gallavotti and E. G. D. Cohen, "Dynamical ensembles in nonequilibrium statistical mechanics," Phys. Rev. Lett. **74**, 2694–2697 (1995b).
[44]G. C. Papanicolaou and W. Kohler, "Asymptotic theory of mixing stochastic ordinary differential equations," Commun. Pure Appl. Math. **27**, 641–668.
[45]J. R. Dorfman, *An Introduction to Chaos in Nonequilibrium Statistical Mechanics*. Cambridge Lecture Notes in Physics (Cambridge University Press, 1999).
[46]H. Risken, *The Fokker-Planck Equation: Methods of Solutions and Applications*, 2nd ed. (Springer Verlag, Berlin, Heidelberg, 1989).
[47]R. Kubo, M. Toda, and N. Hashitsume, *Statistical Physics II. Nonequilibrium Statistical Mechanics*, Springer Series in Solid-State Sciences, Vol. 31 (Springer, Berlin, Heidelberg, 1985).
[48]P. Grigolini, "A Fokker-Planck equation for canonical non Markovian systems: A local linearization approach," J. Chem. Phys. **89**, 4300–4308 (1988).
[49]M. Bianucci, P. Grigolini, and V. Palleschi, "Beyond the linear approximations of the conventional approaches to the theory of chemical relaxation," J. Chem. Phys. **92**, 3427–3441 (1990).
[50]M. Bianucci and P. Grigolini, "Nonlinear and non Markovian fluctuation-dissipation processes: A Fokker-Planck treatment," J. Chem. Phys. **96**, 6138–6148 (1992).
[51]P. Prasad and R. Ravindran, *Partial Differential Equations* (John Wiley & Sons, New York, 1985).
[52]M. Bianucci, "Using some results about the Lie evolution of differential operators to obtain the Fokker-Planck equation for non-Hamiltonian dynamical systems of interest," J. Math. Phys. **59**, 053303 (2018).
[53]J. A. Revelli, C. E. Budde, and H. S. Wio, "Diffusion in fluctuating media: First passage time problem," Phys. Lett. A **306**, 104–109 (2002).
[54]V. G. Kulkarni and E. Tzenova, "Mean first passage times in fluid queues," Oper. Res. Lett. **30**, 308–318 (2002).
[55]N. V. Kampen, "First-passage problems," in *Stochastic Processes in Physics and Chemistry,* North-Holland Personal Library, 3rd ed., edited by N. V. Kampen (Elsevier, Amsterdam, 2007), Chap. XII, pp. 292–325.
[56]M. Ding and G. Rangarajan, "First passage time problem: A Fokker-Planck approach," in *New Directions in Statistical Physics: Econophysics, Bioinformatics, and Pattern Recognition*, edited by L. T. Wille (Springer Berlin Heidelberg, Berlin, Heidelberg, 2004), pp. 31–46.
[57]A. J. F. Siegert, "On the first passage time probability problem," Phys. Rev. **81**, 617–623 (1951).
[58]B. Lindner, "Moments of the first passage time under external driving," J. Stat. Phys. **117**, 703–737 (2004); arXiv:cond-mat.
[59]A. T. Wittenberg, "Are historical records sufficient to constrain enso simulations?" Geophys. Res. Lett. **36**, 0–0 (0000).
[60]H. Kramers, "Brownian motion in a field of force and the diffusion model of chemical reactions," Physica **7**, 284–304 (1940).
[61]A. M. van den Brink and H. Dekker, "Reaction rate theory: Weak- to strong-friction turnover in Kramers' Fokker-Planck model," Phys. A Stat. Mech. Appl. **237**, 515–553 (1997).
[62]M. Bianucci, "Ordinary chemical reaction process induced by a unidimensional map," Phys. Rev. E **70**, 026107–1–12617–6 (2004).
[63]C. Gardiner, *Stochastic Methods*, Springer Series in Synergetics, Vol. 20 (Springer-Verlag, Berlin Heidelberg, 2009).
[64]S. McGregor, A. Timmermann, and O. Timm, "A unified proxy for ENSO and PDO variability since 1650," Clim. Past **6**, 1–17 (2010).
[65]F.-F. Jin and J. D. Neelin, "Modes of interannual tropical ocean-atmosphere interaction a unified view. Part I: Numerical results," J. Atmos. Sci. **50**, 3477–3503 (1993).
[66]J. D. Neelin and F.-F. Jin, "Modes of interannual tropical ocean-atmosphere interaction a unified view. Part Ii: Analytical results in the weak-coupling limit," J. Atmos. Sci. **50**, 3504–3522 (1993).
[67]P. Grigolini, "The projection approach to the Fokker-Planck equation: Applications to phenomenological stochastic equations with coloured noises," in *Noise in Nonlinear Dynamical Systems*, Vol. 1, edited by F. Moss and P. V. E. McClintock (Cambridge University Press, Cambridge, England, 1989) Chap. 5, p. 161.
[68]B. Carmeli and A. Nitzan, "Non-markovian theory of activated rate processes. I. Formalism," J. Chem. Phys. **79**, 393–404 (1983).
[69]W. Moon and J. S. Wettlaufer, "A stochastic perturbation theory for non-autonomous systems," J. Math. Phys. **54**, 123303 (2013).